THE PENNSYLVANIA STATE UNIVERSITY
SCHREYER HONORS COLLEGE

DEPARTMENT OF AEROSPACE ENGINEERING

Measurement of Solid Propellant Burning Rates Using Photodiode Arrays

MATTHEW JAMES STEVENS
SPRING 2022

A thesis
submitted in partial fulfillment
of the requirements
for a baccalaureate degree
in Aerospace Engineering
with honors in Aerospace Engineering

Reviewed and approved* by the following:

Richard A. Yetter
Professor of Mechanical Engineering
Thesis Supervisor

Kenneth Brentner
Professor of Aerospace Engineering
Honors Adviser

* Electronic approvals are on file.

ABSTRACT

The measurement of solid propellant burning rates provides critical information for the successful design of solid rocket motors. By knowing the burning rate of a propellant across a range of pressures, the mass flow through the motor can be determined through mass conservation. Typical burning rate determination methods require extensive preparation of propellant samples, significant post processing work, or a combination of both. This study focuses on the development of a photodiode array measurement system for tracking the burning surface of solid propellant in a strand burner. Pressures in the range of 100-1000psi were tested with both a heterogenous propellant, Advanced Solid Rocket Motor Propellant (ASRM), and a homogenous propellant, JA2. Tests were completed at The Pennsylvania State University's High Pressure Combustion Laboratory (HPCL). A 16-element photodiode array was acquired and supporting circuitry and software was developed to process the output signals from the photodiodes and produce a burning rate. Final rates were very close to those determined using the more traditional camera-based method, with an average percent difference across all tests of 3.16%. ASRM propellant had slightly higher percent differences, with an average of 4.29% while the JA2 propellant had an average of 2.03%. The differences in flame structure of the JA2 and ASRM propellants are reflected in the outputs of the photodiodes, and the increased variation, or "flickering" of the ASRM is thought to be a potential cause of the increased percent differences. The JA2 was shown to exhibit an asymptotic decrease in radiance along the burning direction of its flame structure, while the ASRM had a more linear decrease.

An amplification PCB was developed for the photodiodes along with MATLAB code to automatically process output data and determine burning rates. A linear actuator was acquired

and mounted with an IR LED to simulate a burning surface for initial testing of the system. Various methods for determining burning rate from the photodiode outputs were compared. It was found that a threshold-based approach of the voltage outputs along with a regression line through the position-time plot of the burning surface provided the most accurate burning rates.

TABLE OF CONTENTS

LIST OF FIGURES

LIST OF TABLES

ACKNOWLEDGEMENTS

My time at the High Pressure Combustion Laboratory and Research East facilities has deepened my interest in propulsion and combustion technologies. I would like to thank Dr. Richard Yetter and Dr. Eric Boyer for providing an environment where I could learn more about these areas of research, helping me troubleshoot technical issues with my research, and guiding the design process of the instrument discussed in this paper. I would also like to thank David Drewniak for showing me how to use the strand burner at HPCL and helping me solve the many problems encountered. Thank you to my peers Steven Budzinski and Victor Baran for helping me work through problems at our research meetings and for providing general help in the months leading to this thesis.

Chapter 1 Introduction

1.1 Burning Rate Fundamentals

Burning rate is a primary performance characteristic of rocket propellants and is critical for the successful design of a solid motor. Burning rate is the speed at which the ignited surfaces of the propellant regress normal to the surface and is strongly dependent on the pressure of the environment, as described by St. Robert's Law [2]

$$r = ap^n \qquad (1.1)$$

where a is the temperature coefficient, p is the pressure, and n is the pressure exponent. The values of a and n are determined experimentally and are typically only applicable over specific pressure ranges.

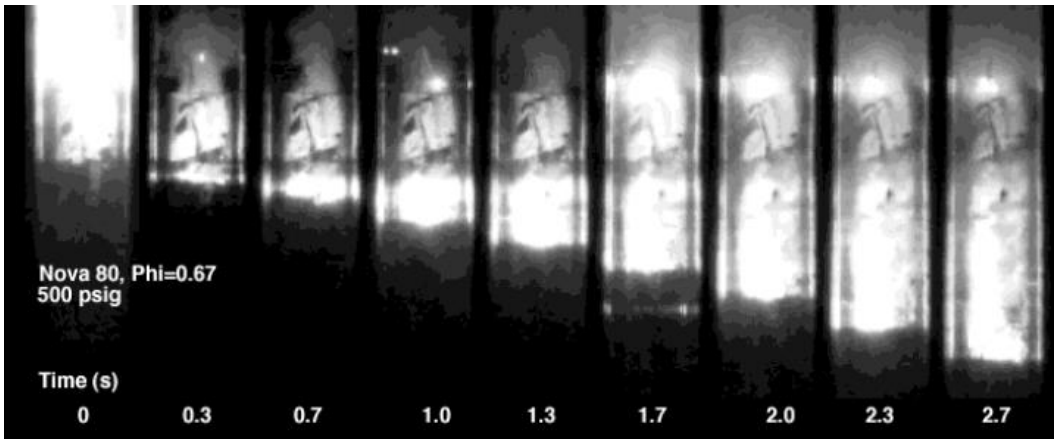

Figure 1. Burning surface regression of propellant strand [11]

Propellant burning rates are typically measured in a pressure-controlled environment that allows for the burning surface to be tracked. Figure 1 shows the regression of a typical propellant sample at elevated pressure. As time progresses, the burning surface of the propellant moves downward at a roughly constant rate.

1.2 Burning Surface and Flame Properties

In order to optically measure burning rates of solid propellants it is important to know the wavelengths of radiant energy and structure of the flame produced above the propellant. Based on the light wavelengths, an appropriate image sensor can be selected that has a response covering this range.

Directly above the burning surface of a propellant strand, a combustion flame structure forms. A schematic of this flame structure for typical composite and double base propellants are shown in Figure 2.

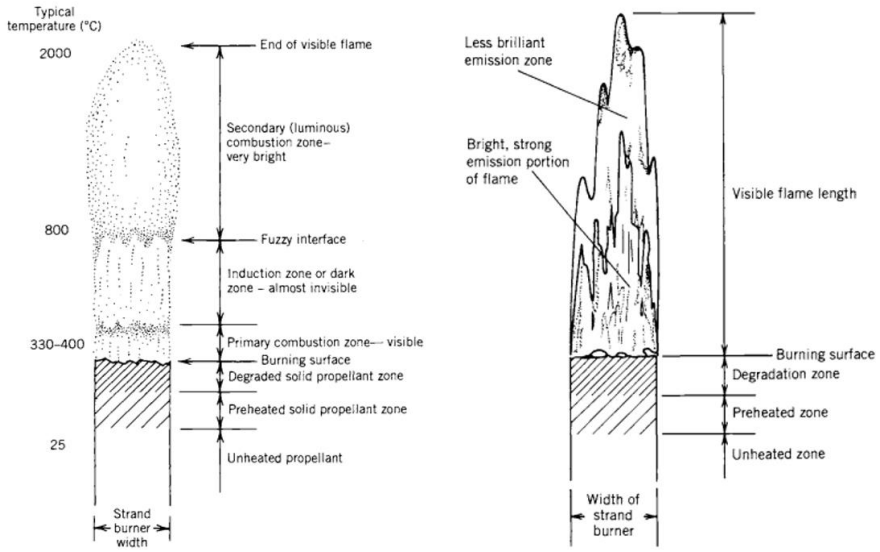

Figure 2. Flame structure of double base (left) and composite (right) propellants [4]

For propellants consisting of a homogenous mixture of two explosives, known as double-base, the propellant flame appears homogeneous and varies little in the radial direction. Just above the propellant burning surface, a dark zone forms that is nearly transparent. For composite propellants, consisting of a powdered metal fuel, crystalline oxidizer, and a binder, the flame

structure varies significantly in the radial direction and appears to thin out as the flow progresses axially. A bright flame forms at the burning surface and remains attached with no dark zone [4].

As shown by S. T. Thynell, the radiant energy in the flame region for an aluminum/ammonium perchlorate/hydroxyl-terminated polybutadiene (Al/AP/HTPB) propellant varies significantly from the unburned propellant zone to the flame [1]. Specifically, the radiance of the burning surface is significantly greater than that of the degradation zone or the downstream flame region.

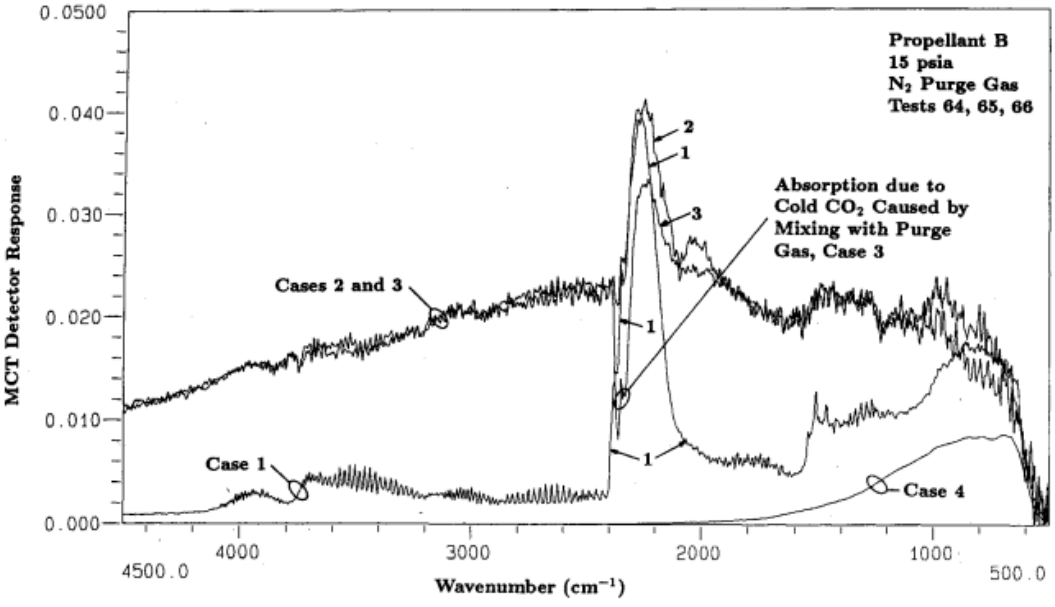

Figure 3. Combustion product emissions of an Al/AP/HTPB propellant strand [1]

Figure 3 shows the differences in recorded emission energy from a few test cases described below:

Case 1 – Combustion products flowing over unburned propellant.

Case 2 – Combustion products flowing over an ignited surface.

Case 3 – The propellant burning surface.

Case 4 – Unburned propellant surface.

For case 4, the MCT detector response is nearly zero in the 5000-2400 cm^-1 wavenumber range. Case 1 shows a slightly higher response at about 0.001 to 0.005 in this same region. For cases 2 and 3, the detector response rises significantly to between 0.011 to 0.024.

The 5000-2400 cm^-1 (2000-4166.67nm) wavenumber range shows significant variations in radiant energy outputs between the unburned propellant, burning surface, and exhaust, allowing for them to be distinguished more easily. This wavenumber range was proposed by Thynell to be used for measuring flame spreading along the surface of propellants containing a significant aluminum content and was a primary motivator for the research work covered in this paper.

1.3 Research Objectives

Experimental methods for measuring burning rate are critical to characterizing propellants for use in solid rocket motors. Importantly, these methods should be quick to set up and efficient at post-processing data to determine a usable burning rate value. The goal of this research is to develop a new photodiode-based instrument to measure burning rates of solid propellant strands. The specific goals include:

- Design amplification circuitry to convert photodiode output signals into voltages readable by standard computer data acquisition systems
- Write post processing code to determine burning rates from the recorded output signals of the photodiodes

- Test the photodiode-based measurement system with heterogenous and homogenous propellant strands and compare the accuracy of burning rate measurements to traditional methods

Chapter 2 Background

2.1 Current Burning Rate Measurement Techniques

The following are current measurement methods for determining burning rates from solid propellants. This list is not exhaustive and these methods were selected as they are two of the most common.

2.1.1 Crawford Strand Burning Bomb

Strand burners make use of a small piece of propellant between 10mm to 150mm in length that is burned under controlled conditions to determine a burning rate. The propellant strand is inhibited on its sides to isolate the burning surface to just the top surface. Thin wires are passed through the sides of the propellant at a known spacing, perpendicular to the burning direction. These wires have current run through them during testing and when the burning surface melts through the wires the stopping of current can be recorded. The spacing between the wires divided by the time delay between the melting of the wires yields a burning rate. The propellant strands are typically placed in an enclosed chamber, called a Crawford bomb, and elevated to high pressures to simulate solid motor conditions [8].

While this method is simple, it requires additional preparation work of the propellant samples by drilling holes in their sides and measuring wire spacing. The number of wires that can fit on a propellant sample is limited which results in large time intervals, thereby yielding average burn rates. The Crawford Strand Burning Bomb burning rate measurement technique is

fairly simple to implement, can achieve accuracies on the order of 2-3% [9], but requires significant preparation of the propellant samples prior to testing.

2.1.2 High Speed Camera

The use of still photography or a video camera to record burning rate relies on the light emissions from the burning propellant. Typically, a clear window on the side of the combustion chamber is used to view the flame front as shown in Figure 4.

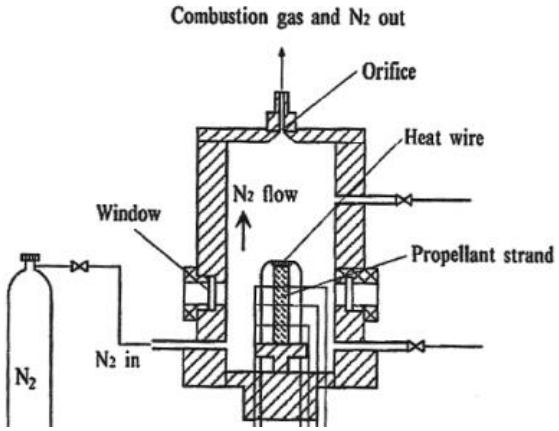

Figure 4. Crawford Bomb with Window for Camera Measurement [9]

A Crawford Bomb is typically used to control the combustion pressure and a camera is placed on the outside of the chamber, normal to the viewport. A constant flow of nitrogen is passed from the bottom to the top of the chamber to prevent combustion products from blocking the view of the burning surface. The video output from the camera is then recorded and processed on a computer. The output video often looks similar to Figure 1. The progression of the burning surface from frame to frame can be compared to a known measurement in the camera field of view and used to determine a burning rate.

The high speed camera method does not require additional preparation of the burning strands, and is fairly simple to set up. However, the cameras used are often quite large and must be placed on the outside of the chamber, requiring a more complex Crawford bomb design with a window. In addition, the processing of the data to determine a burning rate is tedious and time consuming. Camera-based methods produce burning rate measurements with an error typically +/- 3% [10].

Chapter 3 Instrumentation Design and Experimental Setup

3.1 Data Acquisition System

In order to produce a burning rate from photodiodes, the signal output from the photodiode array must be recorded by a data acquisition system. The goal for the data acquisition system is to record the outputs from the photodiodes in real time during burning of the propellant samples. Figure 5 shows the layout of the data acquisition system, consisting of the photodiode array, amplification circuitry, data acquisition hardware, and Windows PC. For each of the 16 diodes, a signal output and timestamp were recorded and saved to the computer.

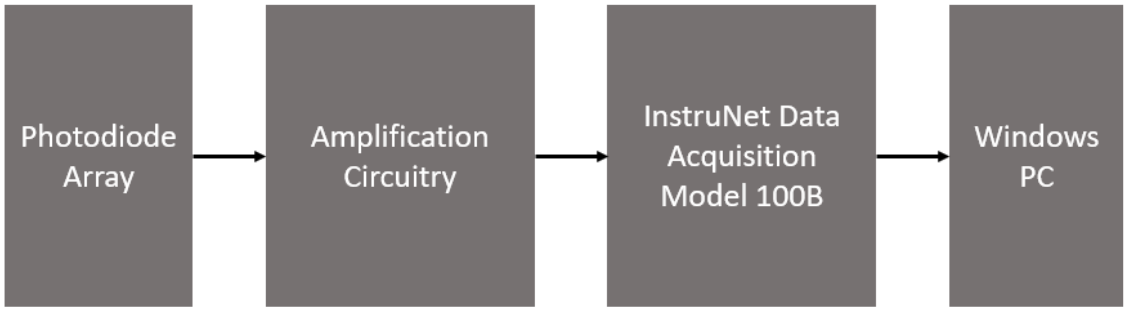

Figure 5. Data Acquisition System

It was determined early on that storing the entire data acquisition system inside a strand burner would add unnecessary complexity to the system. Instead, just the photodiode array and amplifying circuitry were placed in the chamber, with the power supply, InstruNet data acquisition hardware, and windows PC outside the chamber. Power for the amplification circuitry was provided by a standard DC power supply and fed in through 3 wires; one for ground, one for the positive rail, and one for the negative rail. Storing the amplification circuitry and photodiode array together minimized the number of circuit boards that were needed but did

place a constraint on the size of the PCB for the electronics. The InstruNet Data Acquisition Model 100B provided 16 channels with +/-5V, 14 bit, analog input with a +/-1500 μV absolute accuracy.

3.1.1 Photodiode Array

The main requirements for the photodiode array were:

- Should have a spectral response in the wavelength range of 2000-4166.67 nm as proposed by Thynell [1]
- Should be compact enough to fit inside the 3in diameter of existing pressure chambers at the HPCL
- Be relatively low cost as the chance of damage while in the combustion chamber is rather high.

The A2V-16 Planar Diffused Silicon Photodiode Array by OSI Optoelectronics was determined to be the best fit for the above requirements. While its spectral response is limited to 1100nm, it was reasonably priced compared to far-infrared units and would likely still be good enough for initial testing of the amplifying circuitry and overall testing process.

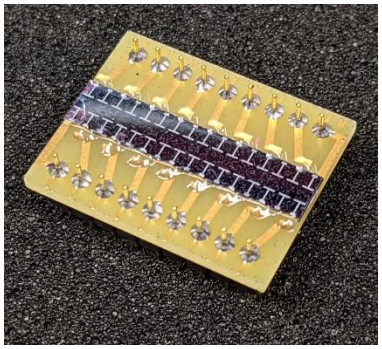

Figure 6. A2V-16 Photodiode Array

3.1.2 Amplification Circuitry

The photodiodes output a current based on the irradiance of the light on their exposed surface. The available data acquisition units read a voltage, so the current output from the photodiodes must be converted to a voltage and amplified to a readable level. A transimpedance amplifier provided the ability to convert the current outputs into a voltage and amplify this signal.

The relationship between the input current and output voltage was derived for the transimpedance amplifier by solving a Kirchhoff's Current Law (KCL) equation at the node where the feedback and input paths connect, as shown in Figure 7. Equating the feedback current with the input current and solving for the output voltage resulted in the following relationship:

$$V_{out} = -I_{in} \times R_1 \qquad (1.1)$$

Where I_{in} is the current output of the photodiodes and R_1 is the feedback resistor value. Using this equation, it is seen that a negative voltage output will be produced, which could be amplified with a gain of -1 using an inverting amplifier to achieve a positive output. However, the InstruNet Data Acquisition hardware can read negative voltages so this was not implemented.

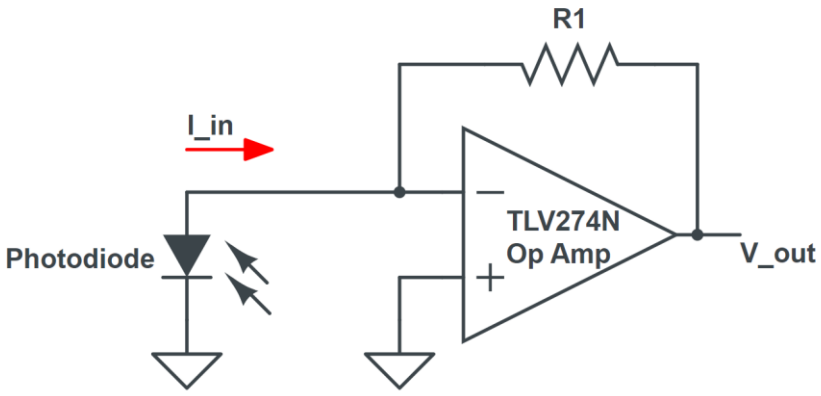

Figure 7. Transimpedance Amplifier Schematic Created in Circuit Lab [13]

Photodiodes produce an output current, or photocurrent, linearly proportional to the illuminance and dependent on the wavelength of the light reaching them. This current flows from cathode to anode, in the direction on the I_{in} arrow in the diagram above. The photodiode array provided a common cathode and 16 anodes, one for each photodiode. The common cathode was connected to ground, putting the photodiode in a zero-bias state, known as Photovoltaic Mode. Alternatively, photoconductive mode requires a voltage bias on the photodiodes. Photovoltaic mode was selected over photoconductive because it eliminates the need for additional circuitry elements to produce the voltage bias, minimizes responsivity, and the readily available photodiode arrays were optimized for photovoltaic mode by the manufacturer. Additionally, minimizing responsivity was desired as the illuminance of the propellant was estimated to be very bright and it was desired to keep the photodiodes in their linear operation range.

The schematic in Figure 7 served as the basis for the amplification circuitry that was used for the A2V-16 photodiode array. For the transimpedance op-amps, the TLV274IN chip was selected because of its compact size at 4 circuits per chip, rail to rail output which minimizes required input voltage, and low cost. The transimpedance amplification circuit for four of the

photodiodes is shown in Figure 8. The schematic was drawn using KiCad, a free software package for designing and simulating electronic circuits.

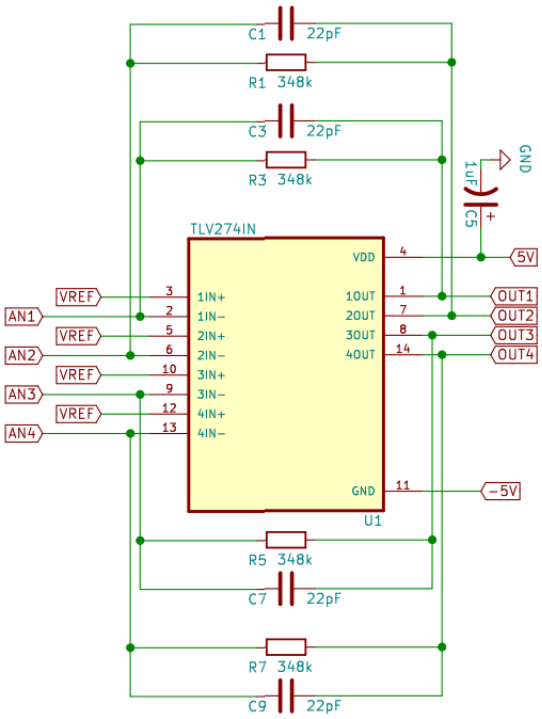

Figure 8. Schematic of transimpedance op amp circuit for one TLV274IN chip

Each TLV264IN chip provides amplification for 4 diodes, requiring 4 chips to amplify all 16 diodes. AN1 – AN4 are the current outputs from the photodiodes and OUT1 – OUT4 are the amplified voltage outputs. The feedback resistors (R1, R3, R5, R7) set the gain of the amplifiers. Gain was measured in V/mA and is calculated by the equation below

$$\mathrm{G} = \frac{V_{out}}{-I_{in}} = -R_1 \qquad (1.1)$$

Different resistor values were tested to determine which gain value would produce photodiode voltage outputs that did not saturate the InstruNet Data Acquisition module's +/-5V range. Initial tests to determine the appropriate gain value are shown in Appendix E.

The amplification circuit was powered using +9V, -9V, and ground wires from a Tektronix PS280 DC power supply. These voltages were then regulated to +/-5V using the circuitry in Figure 9 and supplied to the transimpedance op-amps. +/-5V was selected as this is the maximum input range for the InstruNet Data Acquisition Model. A 7805 was used to regulate the positive rail and a 7905 was used for the negative rail.

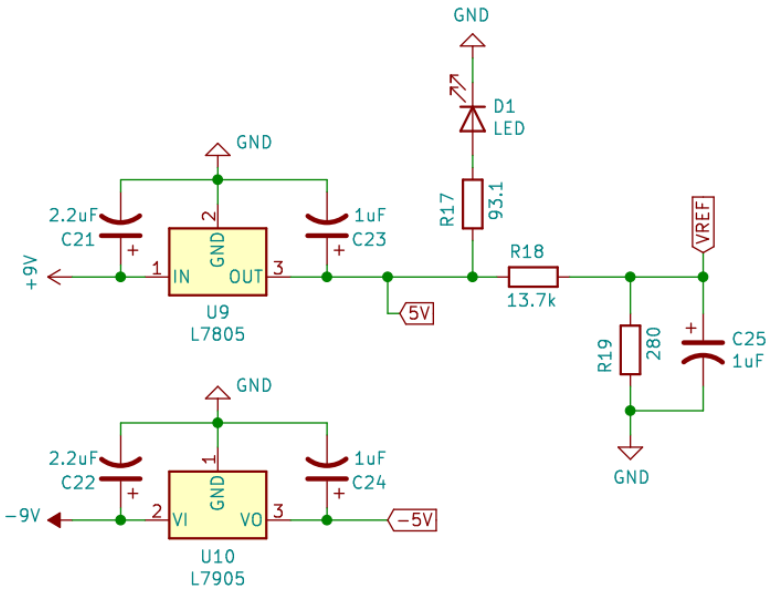

Figure 9. Power circuit for amplification PCB

An LED was also included on the board to improve visibility when viewing the board from outside the pressure chamber. The LED was chosen to be 470nm, corresponding to a low responsivity on the photodiode array, to ensure it would not interfere significantly with the photodiode array output.

The PCB for the photodiode array amplification circuitry was also designed in KiCAD. Ceramic capacitors were selected to withstand the high pressures expected in the strand burner. Through hole components were selected for ease of soldering. Because of the larger component size, this resulted in fairly densely packed traces on both sides of the PCB. A ground plane was

used on the top and bottom of the PCB to reduce electrical noise. The final PCB was produced by OSH Park. The final board with components soldered is shown in Figure 10.

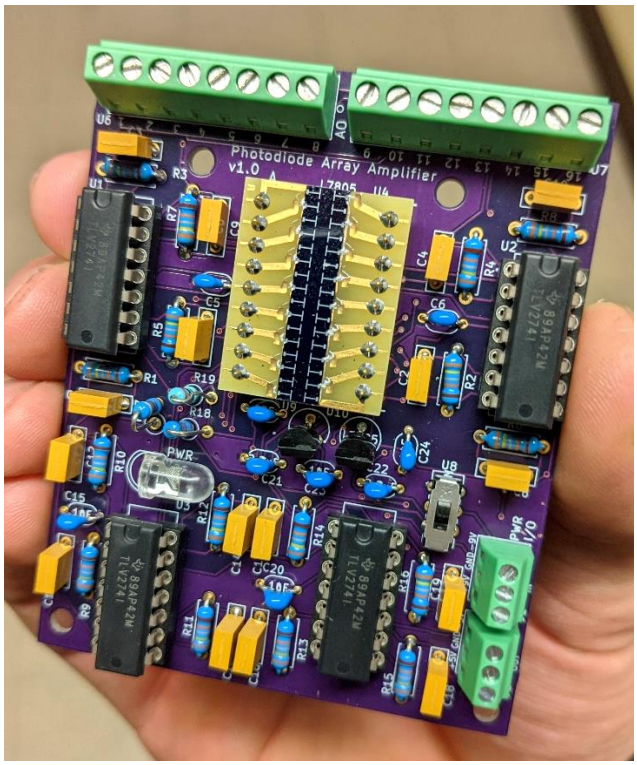

Figure 10. Photodiode amplification board with components soldered

Power is delivered through screw terminals on the side, and the 16 photodiode voltage outputs are on the top of the board. An additional 3 terminals breakout +5V, -5V, and GND from the voltage regulators should they be needed for powering additional electronics in the future.

3.1.3 Photodiode Array Aperture

To limit the visibility of the burning surface for each of the photodiodes on the array, an aperture was designed to reduce the visibility angle. By reducing the visibility angle of each

diode, the output signals of the diodes were more separated, preventing the signals from saturating as soon as the propellant burning was initiated.

The aperture had 16 evenly spaced slits for each of the photodiodes in the array. The visibility angle of the didoes as measured in the CAD was 11.9 degrees as shown in the diagram below.

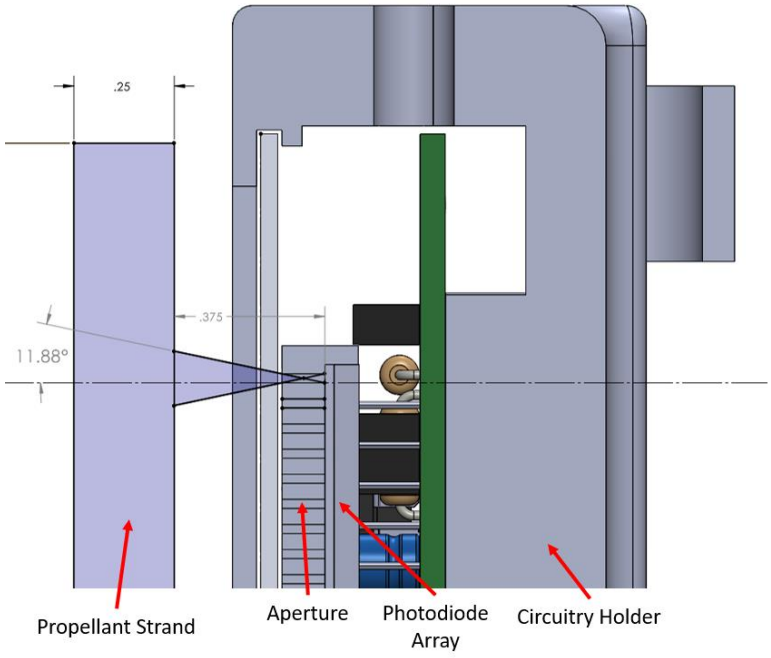

Figure 11. Visibility angle of photodiode aperture

The aperture piece was 3D printed and designed to press fit directly onto the photodiode array. To ensure the aperture was opaque to the infrared radiation emitted by the propellant, it was covered in a single sheet of tinfoil. The tinfoil was fastened using glue and was cut in the locations of the slits.

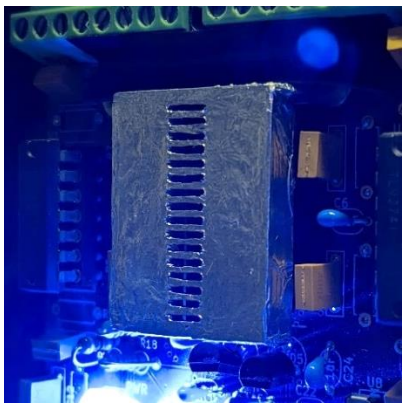

Figure 12. Photodiode aperture covered in tin foil

3.1.4 Photodiode Circuitry Holder

A holder for the photodiode amplification circuitry was needed to position the photodiode array elements parallel to the strand of propellant. It was also important that the holder held the array steady throughout the burning processes and fit within the 3in inner diameter of the chamber. A 3D printed holder was designed in SOLIDWORKS to meet these requirements.

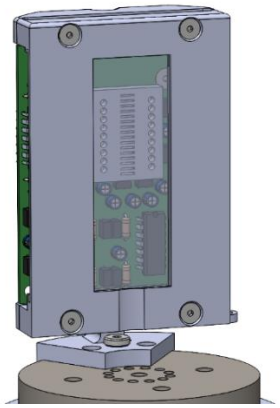

Figure 13. Holder CAD model for photodiode circuitry

3D printing was selected to allow for rapid iteration of the design. Polylactic acid (PLA) filament was selected for the printing material. While PLA is not as heat resistant as metal, it can

be easily replaced and serves to insulate the electronics from the metal chamber walls, preventing any accidently shorting.

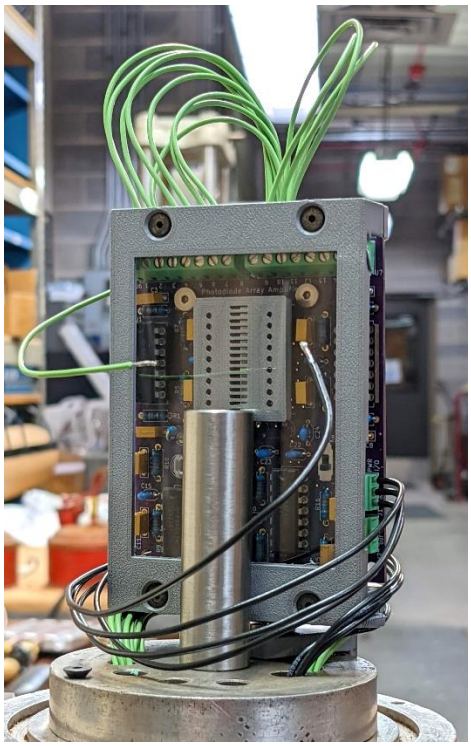

Figure 14. Circuitry holder for the photodiode array

The holder includes a front slot for a quartz microscope slide to prevent soot from collecting on the PCB, wire guides to securely route signal and power wires, and a removable front to allow for easy access to the PCB. The front of the holder could be easily re-printed to accommodate different sized microscope slides.

3.2 Post-Processing Code

To efficiently process data from strand burner tests, a MATLAB script was developed to determine burning rate from the photodiode output data. Voltage outputs for 11 of the

photodiodes were recorded at 1000hz for about 10 seconds per test, resulting in over 100,000 data points per test. The goals for the MATLAB script were to smooth the voltage outputs to improve readability, determine a burning rate, and produce plots of voltage-time for each channel and position-time of the burning surface.

The voltage outputs of each photodiode were saved to a Windows PC using software provided by InstruNet. A single CSV file was produced with columns for time and voltage of each of the channels. The CSV file was then input to MATLAB and trimmed to the region of the burn, corresponding to a dip in the voltage outputs.

Smoothing of the output signals was accomplished using MATLAB's built-in "smooth" function, which incorporates a moving average. A span of 10-30 data points was used for each test, although this did not have a significant effect on the determined burning rate and was mainly for visibility on the plots.

Movement rates of the burning surface were determined by setting a voltage threshold and marking the time when each output signal crossed this threshold. Because the spacing of the diodes is know to be 0.0625", this can be divided by the time difference when two adjacent diodes cross the voltage threshold to get a rate.

Burning rate was calculated in a few different ways to determine which method provided values closest to the camera-determined rates. The first method involved finding a rate between each pair of adjacent diodes, and then taking an average to determine what was called the "Threshold-Average" rate. The second method looked at the first and last diodes only, and used the length of the entire array to find a rate, known as the "Threshold, First/Last Action" rate. The third method plotted position-time of the burning surface, performed a linear regression through

the position points, and then found the slope of the line to determine a rate. This was known as the “Threshold, Linear Regression” rate.

To determine the threshold value automatically, all possible threshold values for the voltage-time plot were considered and a corresponding R^2 value for the regression line was produced. The threshold corresponding to the largest R^2 value was used. This method was chosen as burning rates ideally are linear, so the threshold corresponding to the most linear spacing of burning surface positions was expected to provide the most accurate burning rates.

3.3 Instrumentation Testing

To confirm that the photodiode array circuitry and MATLAB post-processing code were functioning properly, a test was developed to simulate a moving burning surface. First, a prototype of the photodiode circuit was built on a breadboard and mounted in a 3D printed enclosure. 4 photodiodes were connected to transimpedance amplifiers and recorded by a Window’s PC running a basic LabView program.

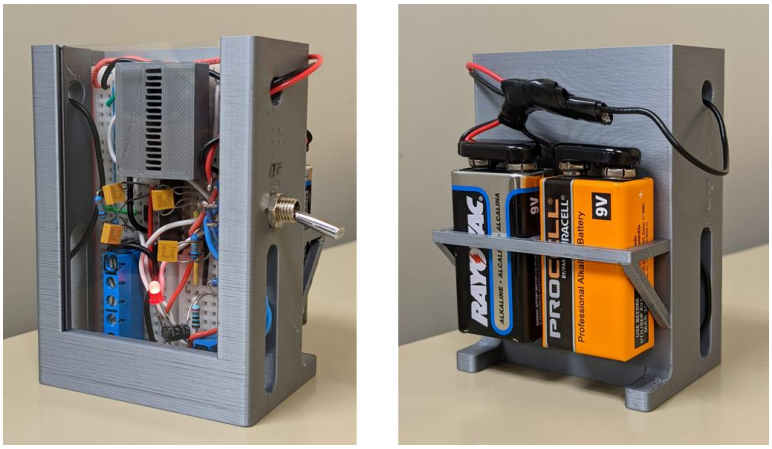

Figure 15. Prototype photodiode amplification circuitry and holder

To simulate a moving burning surface, a linear actuator was acquired and mounted on a 3D printed holder in the vertical position. An LED was mounted to the end of its arm with a 3D printed piece providing a 1mm slit for light to pass through. The LED was chosen to have a 900nm wavelength to ensure it would be registered by the photodiode array.

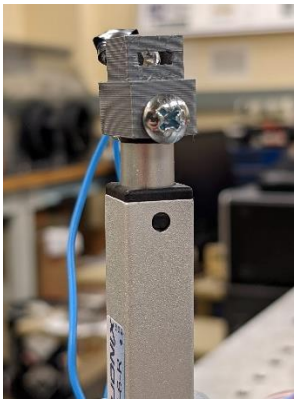

Figure 16. Linear actuator with LED mounted on end

The linear actuator and LED were placed in front of the photodiode array and driven at a known rate using an Arduino Microcontroller. This rate was then compared with the rate measured by the photodiode array.

Figure 17. Test setup for photodiode instrument with linear actuator motion path (red arrow) and LED emission lines representation (orange lines).

The calculated rates from the linear actuator are provided in Appendix C. Overall, the actuator served to validate the photodiode array circuitry and post processing code and showed that reasonable rates could be obtained.

3.4 Experimental Setup

The test setup for capturing photodiode array and camera data consisted of a 3in inner diameter strand burner pressure chamber, propellant holder, camera, and photodiode circuitry as shown in Figure 18.

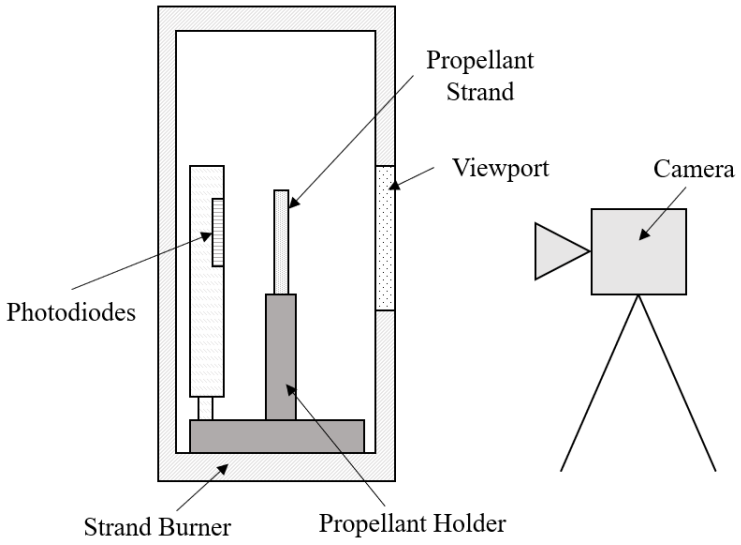

Figure 18. Experimental setup diagram

The camera had visibility of the propellant strand through a glass viewport on the side of the strand burner. The camera was positioned approximately 4ft away from the strand burner.

3.4.1 Strand Burner

The strand burner test setup was located at the High Pressure Combustion Laboratory (HPCL) at Penn State [15]. Inert nitrogen gas was used to pressurized the chamber and pressure was controlled using the valve panel showed in Figure 19.

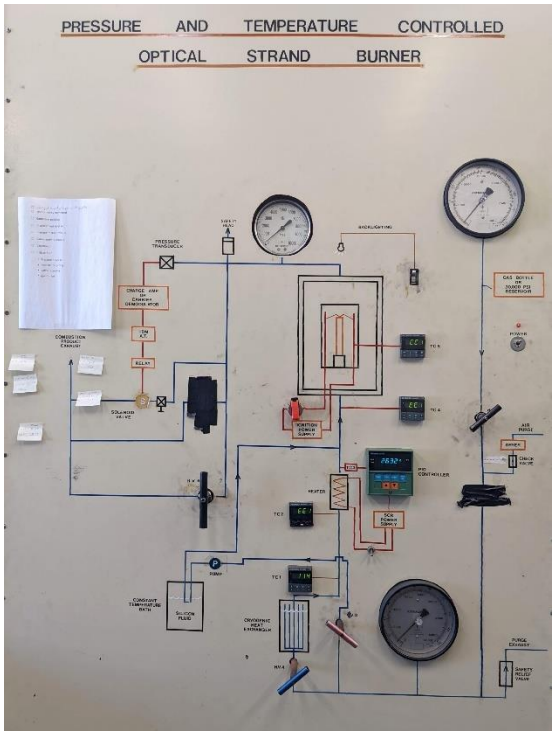

Figure 19. Strand Buner Valve Control Panel

During testing it was important to have a constant flow of nitrogen to remove combustion products out of the chamber and allow the camera and photodiode array to view the burning surface.

The pressure chamber had an inner diameter of 3in and a threaded removable plug where wire pass throughs and circuitry were located. The available wire pass throughs allowed for 4 wires each, allowing for 16 total wires to be sent through the plug. 3 were used for power, 2 for the igniter, and 11 were for the photodiode voltage outputs.

3.4.3 Propellant Holder

The goal for the propellant holder was to securely hold the propellant strand during the burning process. An existing propellant holder was used that had a 0.5in diameter and 0.5in depth hole.

Figure 20. Propellant holder with 0.5in upper hole

To fit the square cross section of the propellant samples into the propellant holder, a 3D printed adapter was made with a circular perimeter and square cavity for the propellant to be placed in.

3.4.4 Propellant Preparation

Two types of propellant were used for testing: Advanced Solid Rocket Motor (ASRM) and JA2. The ASRM propellant was cut into segments of 2in length, and 0.25in x 0.25in cross section. The JA2 was cut into 2in length segments with a 0.25” circular cross section. It was important to measure the propellant samples prior to loading them into the test chamber so that they could be used to calibrate the pixels/length of the burning rate videos.

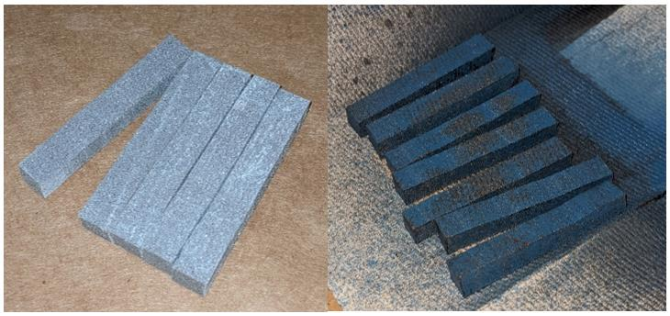

Figure 21. ASRM propellant samples before inhibited (Left), and after spray painted (Right)

The sides of the propellant were inhibited using a combination of black and blue spray paint to ensure only the top burning surface was ignited, leading to a clean regression of a single surface during the burn.

3.4.5 Testing Procedure

The goal for each test was to collect video data of the burning surface, the voltage outputs from the photodiode amplification board, and ensure the test was operated at the proper pressure. The first step was mounting the photodiode holder and amplification circuitry onto the threaded plug. Next, the amplification board had power and output wires connected to its screw terminals. It was important to ensure wires were tightly secured to prevent them from getting caught when threading the plug into the chamber.

Figure 22. Photodiode amplification circuitry mounted on strand burner plug

Next, the propellant sample was loaded into the holder and a 4in section of nichrome wire was passed through a small slit cut in the top surface of the propellant. The nichrome wire was used to ignite the surface when a high current was passed through its length. The threaded plug was then inserted into the chamber and tightened to ensure it formed a proper seal. Next, the chamber was brought up to the desired pressure and the camera and photodiode data recording started. The propellant was then ignited and after burning was completed the data was saved to a USB memory stick.

Chapter 4 Results and Discussion

Strand burner tests were completed with both ASRM and JA2 propellant types at pressures ranging from 100-1000psi. Burning rate was determined in five different ways which are summarized below:

- **Published Data Burning Rate**: Calculated using published temperature coefficient (a) and pressure exponent (n) values at the pressure of each test. Published values for JA2 were provided by Kuo [3] and for ASRM by Cohen [14].
- **Camera Burning Rate**: Calculated from the camera data by dividing a known distance by time of burning
- **Photodiode Threshold, Linear Regression**: Calculated by plotting a regression line through a position time plot of the burning surface. The position was determined by setting threshold values for each of the photodiode channels, and equating a crossing of the threshold to the burning surface passing over that diode
- **Photodiode Threshold, Average**: Calculated by finding a rate between pairs of photodiodes and then taking an average of these rates.
- **Photodiode Threshold, First/Least Action**: Calculated by looking at the first and last diodes and dividing by the entire array length to determine a rate.

A summary of the tests conducted for both propellant types is shown inTable4.

Table 1. Summary of test data from strand burner tests.

						Burning Rates Photodiode-Based (in/s)					
Test #	Propellant	Pressure (psi)	Pressure (MPa)	Burning Rate Published Data (r=a*P^n) (in/s)	Burning Rate Camera - Based (in/s)	Threshold, Linear Regression	Threshold, Average	Threshold, First/Last Action	% Difference Camera/Least Squares	% Difference Camera/Threshold, Average	% Difference Camera/Threshold, first-last action
5	ASRM	100	0.689	0.194	0.154	0.158	0.165	0.176	2.74%	7.08%	13.51%
6	ASRM	200	1.379	0.242	0.238	0.246	0.269	0.281	3.27%	12.19%	16.53%
7	ASRM	400	2.758	0.302	0.301	0.317	0.967	0.396	5.09%	104.98%	27.17%
8	ASRM	800	5.516	0.377	0.339	0.36	0.374	0.399	6.06%	9.87%	16.31%
9	JA2	600	4.137	0.314	0.315	0.318	0.335	0.358	1.04%	6.25%	12.87%
10	JA2	800	5.516	0.397	0.378	0.373	0.394	0.416	1.36%	4.12%	9.55%
11	JA2	400	2.758	0.225	0.222	0.23	0.286	0.255	3.63%	25.29%	13.93%
12	JA2	1000	6.895	0.477	0.439	0.43	0.45	0.483	2.08%	2.47%	9.54%
								Averages:	**3.16%**	**21.53%**	**14.93%**

The fifth column shows the burning rates calculated using published data, the sixth column shows the burning rate determined from the camera, and the highlighted columns show the burning rates determined form the photodiode array using the methods discussed above. Percent differences between the camera burning rate and photodiode determined rates are shown in the last three columns. The linear regression aligned the most closely with the camera-determined rates across all of the tests. The linear regression method was readily determined to be the most accurate method of the three shown and is used in all further discussion.

In general, the percent differences were low, showing that the burning rate determined by the photodiode array aligns well with the camera-determined burning rate. The camera is taken to be the “source of truth” for the burning rate as it is visually calculated and is not as susceptible to variations in brightness as the surface is tracked manually. The average percent discrepancy between the least squares method and the camera determined rates was 3.16% across the tests conducted for JA2 and ASRM propellant. ASRM propellant alone had a higher percent difference of 4.29% while JA2 was only 2.03%.

The burning rate calculated from published data is provided as a reference point. Note that the pressure of each test was not recorded digitally but visually from a pressure gauge on the

strand burner control panel, reducing the accuracy of measurement. The goal for the tests was not to confirm existing published burning rates but to show that the photodiode-based burning rate could align well with a camera-determined rate.

4.1 ASRM Propellant Tests

ASRM strand burner tests were conducted at pressures of 100, 200, 400, and 800 psi. The photodiodes were set at a gain of -0.1V/A, as determined in Appendix E. A camera was used in parallel with the photodiode array to capture video and photodiode voltage output data. Figure 23 shows the photodiode voltage output and position plot for a 100psi test with the ASRM propellant.

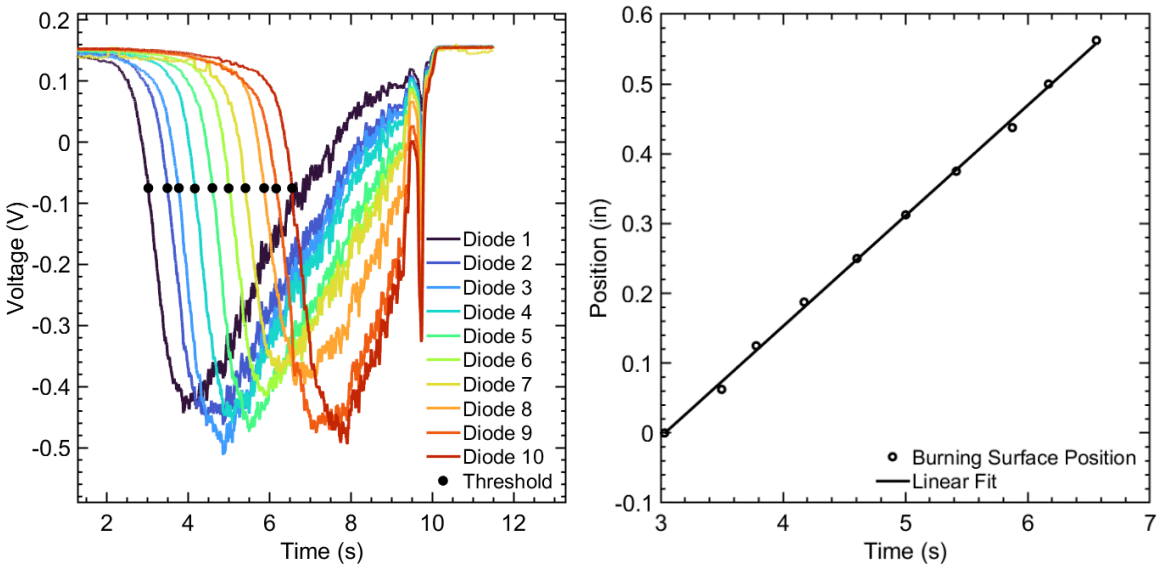

Figure 23. Photodiode voltage output for 100psi ASRM propellant test

Voltage plots for diodes 1-10 are shown along with black markers where the signals cross the threshold value. When a diode output signal crossed this threshold, the burning surface was considered to have "passed" this diode, leading to the position-time plot.

The linear fit of the burning surface position plot had an R^2 value of 0.999, showing a strong linear relationship between burning rate position and time. Taking the slope of the line yields a burning rate of 0.158 in/s. The camera-determined burning rate for the ASRM at 100psi was 0.154 in/s, yielding a 2.7% discrepancy between the photodiode and camera based burning rates.

While the ASRM propellant showed a strong linear correlation between the burning surface position and time, the percent discrepancy between the camera burning rate and photodiode burning rates was typically larger for the ASRM propellant compared to the JA2. One possible explanation for this are the energetic products present in the ASRM exhaust that may interfere with the radiance measured by the photodiodes.

After the ASRM propellant tests, a film of aluminum oxide was observed on the glass slide protecting the photodiodes and circuitry. The collection of exhaust products on the glass diffuses the light, resulting in decreased outputs from the photodiodes. It can be seen in the second half of test 6 that the photodiode outputs seem to “sync up” after about the 6 second mark.

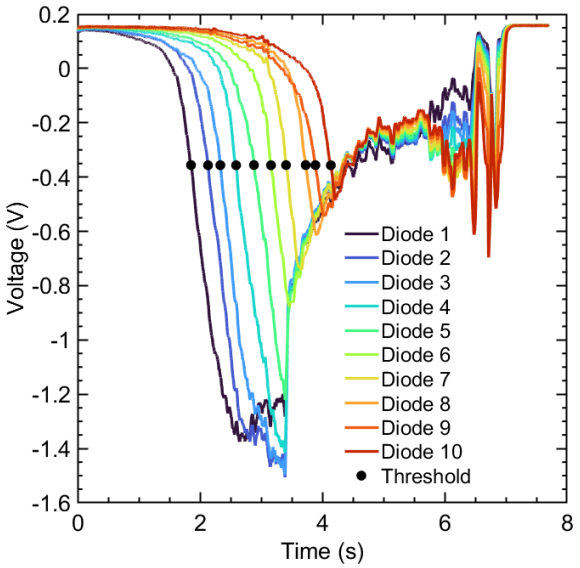

Figure 24. Syncing of photodiode outputs in test 6, ASRM 200 psi

This alignment of the signals could be explained by diffusion of light coming into the photodiode array, causing all of the diodes to perceive similar radiances from the propellant.

Figure 25. Photodiode quartz slide covered with exhaust products

Figure 25 shows the quartz slide after test 6. The collection of exhaust products on the glass, specifically over the photodiode region, likely lead to diffusion of the propellant light leading to indistinguishable photodiode outputs for the second half of the burn. For this test, an acceptable burning rate was still determined based on the spacing of the photodiodes signals for the first half of the burn.

4.2 JA2 Propellant Tests

JA2 strand burner tests were conducted at pressures of 400, 600, 800, and 1000 psi. A gain of -0.1V/A was used for these tests. JA2 had a significantly lower radiance compared to the ASRM propellant, resulting in decreased amplitudes of the photodiode outputs and dimmer camera video. Because it was a homogenous propellant, the flame structure was more uniform than the ASRM and displayed a more even gradient of flame brightness along the burning direction. Figure 26 shows the photodiode outputs and position plot for the JA2 propellant at 800psi.

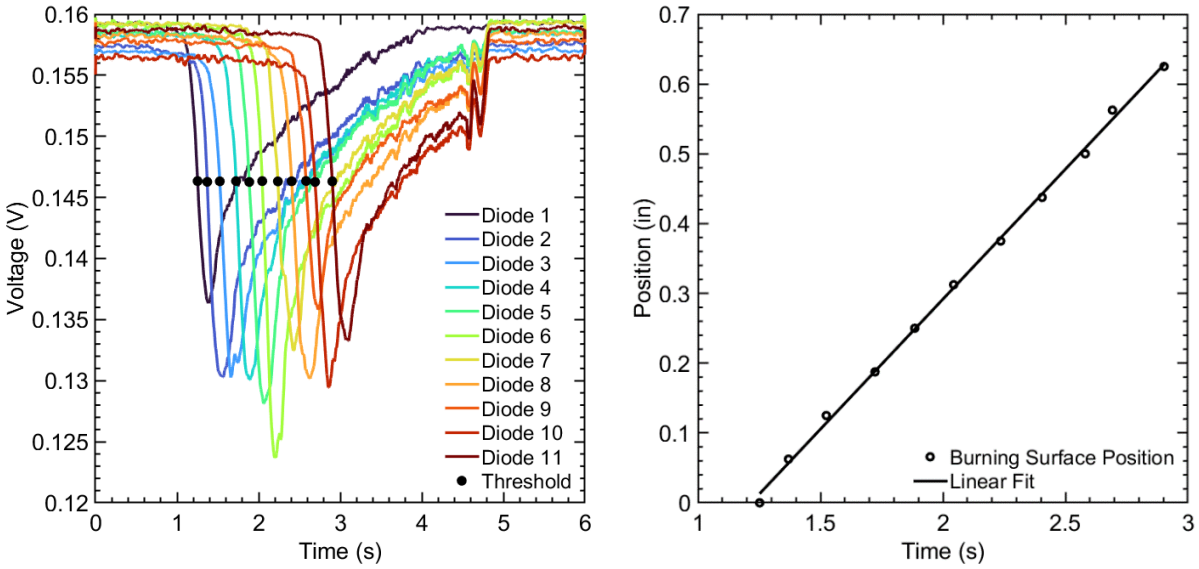

Figure 26. Test 10 photodiode voltage outputs and position time plots for JA2 propellant at 800psi

The linear fit of the burning surface position plot had an R^2 value of 0.999, showing a strong linear relationship between burning rate position and time. Taking the slope of the line yields a burning rate of 0.373 in/s. The camera burning rate was determine to be 0.378 in/s, yielding a 1.36% discrepancy between the two burning rates.

The JA2 strand burner tests had significantly lower voltage outputs from the photodiodes compared to the ASRM propellant. This was expected as the burning surface is typically much dimmer. Ideally, the gains of the transimpedance amplifiers would be increased for the JA2 propellant to allow for the outputs to fill the +/-5V range of the InstruNet data acquisition system, maximizing the resolution of the system.

4.3 Comparison of JA2 and ASRM Photodiode Response

In general, the JA2 burning rates aligned more closely between the camera and photodiode-based rates. This is possibly due to more even flame structure of the JA2 propellant, being a homogenous propellant, compared to the ASRM's composite formulation. Figure 27 (c) and (d) show the ASRM and JA2 flame structures. Having a more even flame structure results in consistent radiance levels along each axial location of the plume. This results in more predictable photodiode voltage outputs, possibly improving the accuracy of the determined burning rate.

The differing flame structures of the JA2 and ASRM propellants is reflected in the outputs of the photodiodes. Figure 27 (a) and (b) shows voltage outputs of the photodiode array for the ASRM and JA2 propellants at 800psi. Both had similar burning rates at around 0.35 in/s.

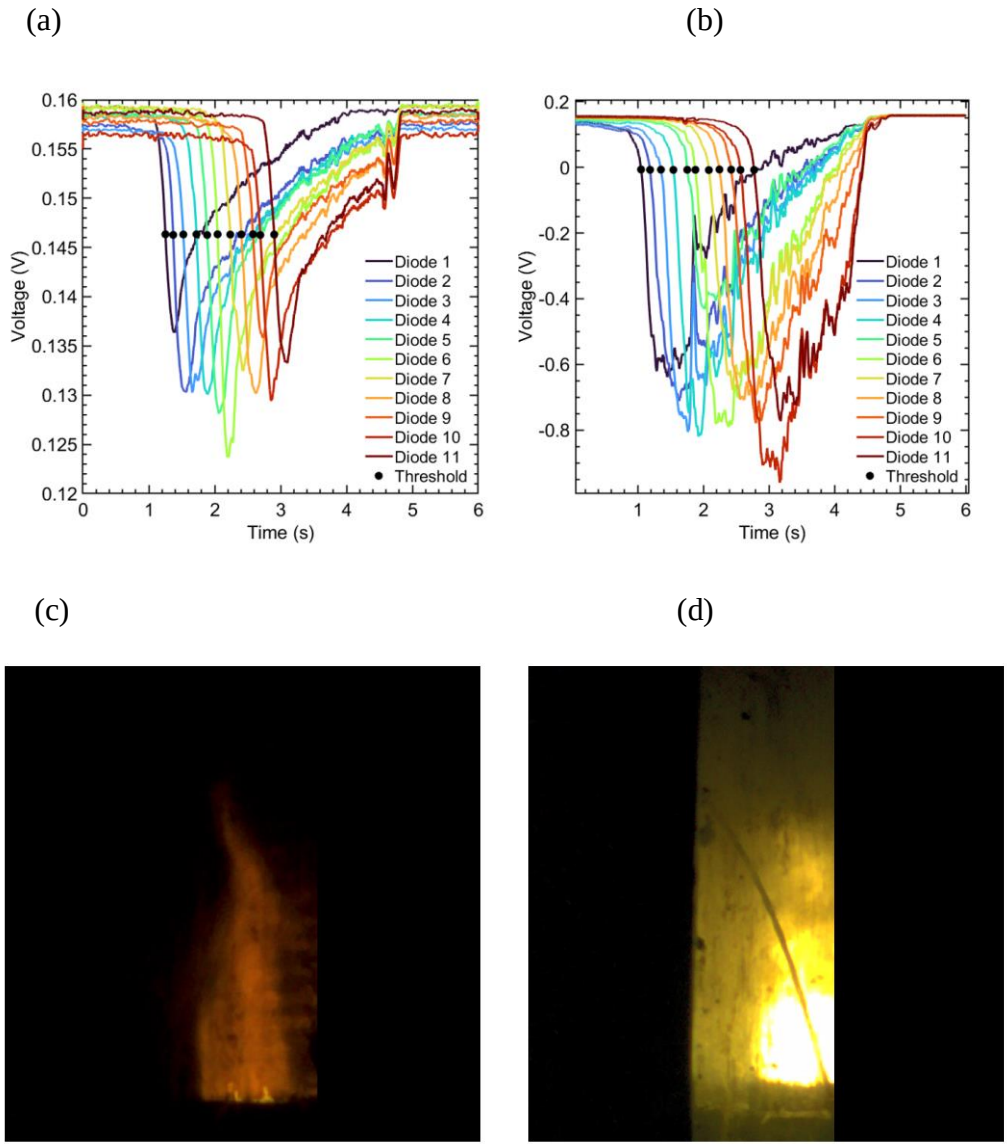

Figure 27. (a) JA2, 800 psi, photodiode response. (b) ASRM, 800psi, photodiode response. (c) JA2 flame at 800psi. (d) ASRM flame at 800psi.

Looking at the diode 1 trace around the 1.2s mark in each plot, the JA2 propellant shows a sharper decrease in voltage output when the burning surface first passes each photodiode. The ASRM photodiode output more gradually decreases initially before achieving a slope similar to that of the JA2. When reaching the minimum in voltage output for each diode, the JA2 shows a sharp trough that ends quickly after the burning surface passes. For the ASRM, the trough is

more sustained and lasts a few hundred milliseconds. This extended photodiode response is expected from the ASRM as there is region of intense radiance above the burning surface due to burning of aluminum particles in the exhaust.

The differences discussed above could possibly be explained by the intense flickering of the ASRM flame. The large fluctuation in the second half of the ASRM burn were likely due to varying radiance levels visible to each photodiode. Also visible in the flame picture from Figure 27 is the consistent region of brightness above the ASRM burning surface which could explain the more sustained troughs in the ASRM photodiode outputs. It is also noted that the photodiode array has a responsivity in the near-IR range, possibly allowing it to reflect additional flame characteristics not visible in the camera video.

For the second half of voltage output curve, after about the 3 second mark, the JA2 displays an asymptotic approach back towards the initial voltage level while the ASRM appears to approach more linearly and with larger fluctuations. Figure 28 shows a linear fit to the ASRM photodiode outputs and a second order polynomial to the JA2 photodiode outputs for the second half of their output curves.

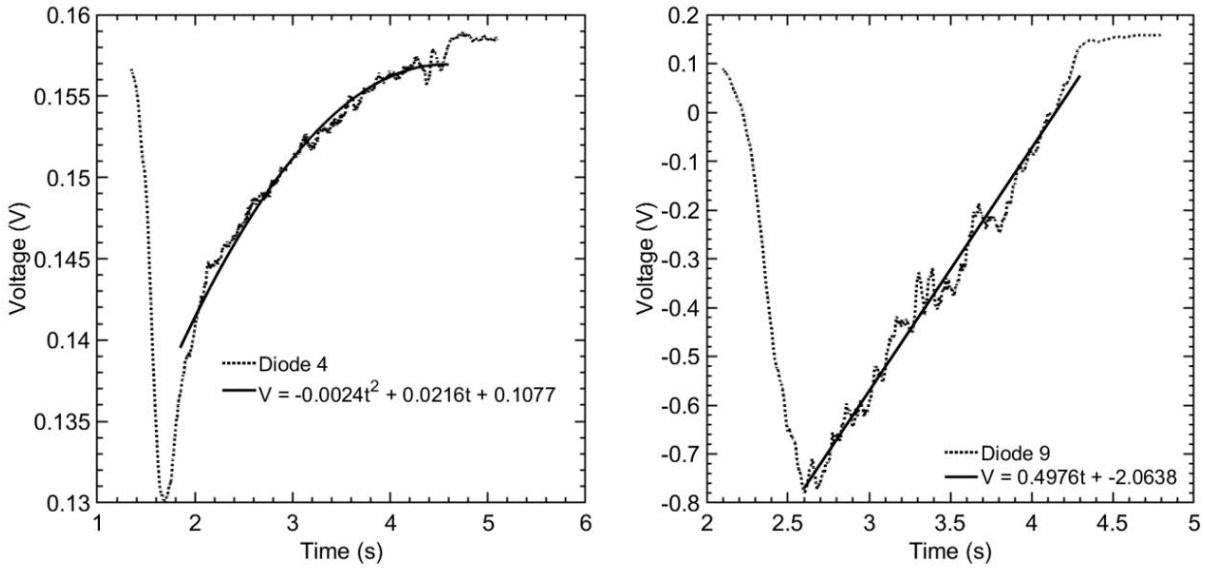

Figure 28. Polynomial fit of JA2 diode output at 800psi (Left). Linear fit of ASRM diode at 800psi (Right).

A single diode was used above for visibility, however, all the diodes from each burn displayed similar behavior. The 800 psi tests were selected for the comparison above as both propellant types had similar burning rates allowing the axis to be scaled similarly. The shape of the photodiode response for the flame structures could be used as an additional metric for characterizing solid propellants. The width of the trough could possibly provide information about the thickness of the burning surface. For the ASRM, the shape of the trough and voltage response due to the flame could possibly be used to calculate burning times of aluminum particles in the exhaust.

4.3 Selecting a Threshold Value for Burning Rate Calculation

The selection of threshold value had little effect on the calculated burning rate from the photodiodes, only affecting final rates by about +/-1%. However, to automate this process a threshold value had to be determined automatically without user input.

To select a "best" threshold value, a rate and corresponding R^2 value from the position-time linear fit was determined for all possible threshold values. The rate with the highest R^2 value was selected as the final rate for each burn. Figure 29 shows the variation in both R^2 and calculated burning rate at each possible threshold value for the JA2 propellant at 1000 psi.

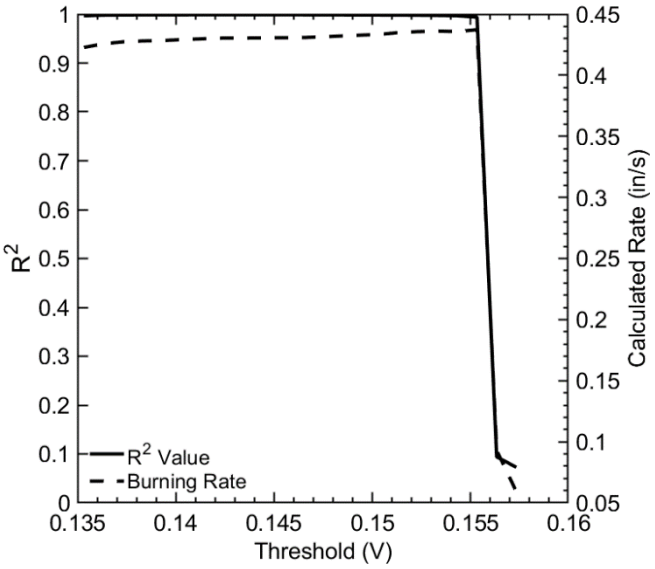

Figure 29. Variation in R^2 and burning rate for each threshold voltage value. JA2 propellant at 1000psi.

The JA2 propellant achieves a maximum R^2 value of 0.999, and maintains a value over 0.995 until a threshold value of about 0.155V. At this point, the spacing of the photodiode voltage signals is not as consistent as shown in Figure 30.

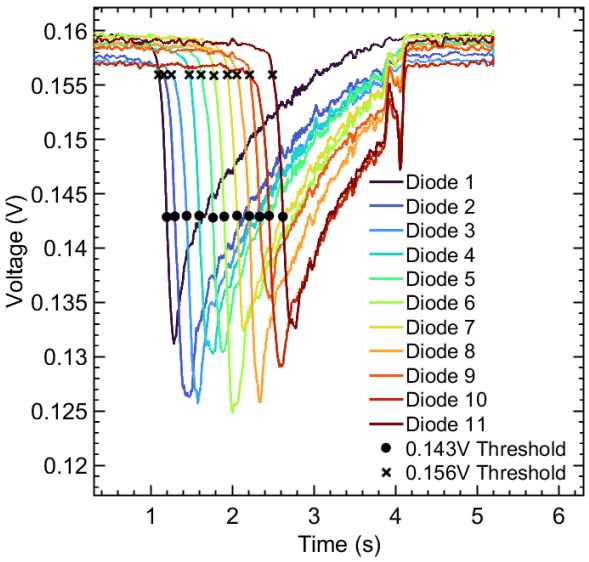

Figure 30. Comparison of marker spacing at different threshold values for JA2

For threshold values over 0.155V, the calculated burning rate deviates substantially as the markers are not very evenly spaced. This occurs in part to the variation in initial voltage of each of the photodiode channels. For threshold value between 00.135 and 0.155 V the calculated burning rates deviates minimally.

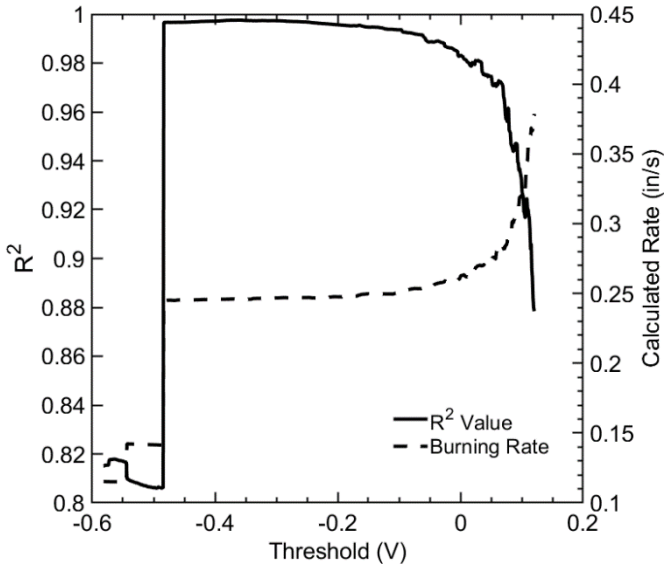

Figure 31. Variation in R^2 and burning rate for each possible threshold value on the photodiode voltage plot. ASRM propellant at 200psi.

Figure 31 shows variation in R^2 and calculated burning rate for the ASRM propellant at 200psi for different threshold values. Deviation in burning rate changes more gradually with varying threshold values. For the lower range of threshold values, the ASRM propellant experienced a significant decrease in the calculated rate, caused by the less distinctive troughs in the voltage-time plots of the photodiodes.

Chapter 5 Conclusions and Future Work

5.1 Conclusions

A 16-element photodiode array data acquisition system was developed to measure emissions from the burning surface and exhaust of ASRM and JA2 propellants to calculate a burning rate. Tests were conducted at Penn State's High Pressure Combustion Lab in the range of 100-1000psi. The burning rates measured from the array showed small differences compared to rates determined from a camera setup, with average percent discrepancies of 2.03% for the JA2 propellant, and 4.29% for the ASRM propellant.

A circuit board was developed with 16 independent transimpedance amplifiers for processing the photodiode current outputs to be read by an InstruNet data acquisition module. An aperture was 3D printed for isolating the response of the diodes and post processing code was developed to automatically calculate burning rate from the photodiode voltage outputs, greatly reducing the processing time typically involved with finding burning rates from strand burner tests.

It was determined that a threshold-based approach for determining when the burning surface passed each diode produced burning rates that aligned most closely with the camera-determined rates. A regression line was plotted through the position-time plot of the burning surface to determine a rate. Selecting the threshold value was accomplished by sampling the space of possible threshold value and selecting the one that produced the lowest R^2 value. It was shown that for most threshold values the calculated burning rates changed very little.

The photodiodes additionally provided information about the plume structure of the propellant strands. The JA2 propellant produced an asymptotic decrease in radiance along its flame, while the ASRM was more linear. This behavior was noted over all of the pressure ranges tested.

5.2 Future Work

The initial goal for this research was to develop an easier to use and faster method for calculating burning rates from solid propellants. The method of using photodiodes has shown a high degree of accuracy in burning rates measured, but to turn this instrument into a commercial product some additional changes could be made. Additional applications for the photodiode array instrument have also been identified, such as characterizing the flame structure of burning propellants, measuring burning times of aluminum particles in the exhaust of aluminized propellants, and measuring the speed of detonation waves in shock tubes. Suggestions for future work related to these topics are listed below:

- Further testing at increased pressures would be useful to see how the sensor responds at increased burning rates. Relationships between burning rate and accuracy of the sensor would be useful for determining the range of burning rates the sensor could function at.
- Adjustable gain values for the amplification board would be useful for testing propellants of various radiances. The JA2 produced a significantly dimmer burning surface compared to the ASRM and could be better optimized with increased gain values, allowing the voltage output to better fill the voltage range of the InstruNet data acquisition module.

- A more robust and precise aperture for the photodiodes should be developed. The current 3D printed adapter was limited in its precision, making it difficult to ensure each photodiode had the same window area for light to reach its surface. Difference in the exposed area of each photodiode can result in changes in the calculated burning rate.
- The photodiode array could be separated from the amplification PCB to reduce the footprint of the sensor inside the chamber. This would allow the sensor to be used in smaller chambers.
- Increase the distance between the photodiode array and the propellant burning surface to reduce the amount of soot that collects on the quartz slide. As shown in some of the ASRM propellant tests, soot from the combustion products would collect on the quartz slide, diffusing the light from the propellant strand. This would cause the photodiode outputs to “sync” and become indistinguishable, reducing the ability to calculate a burning rate.

Appendices

Appendix A Amplification PCB Schematic

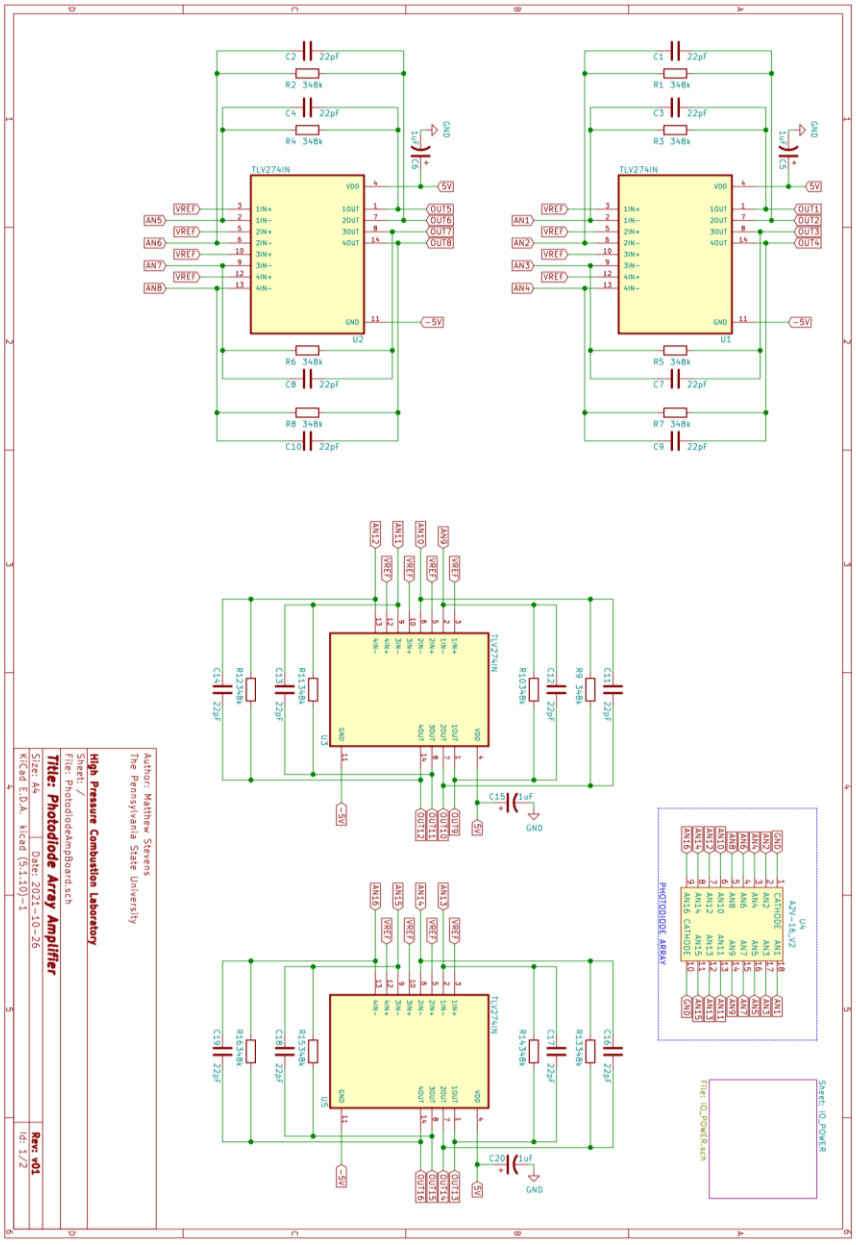

Figure 32. Amplification PCB Schematic Pg.1

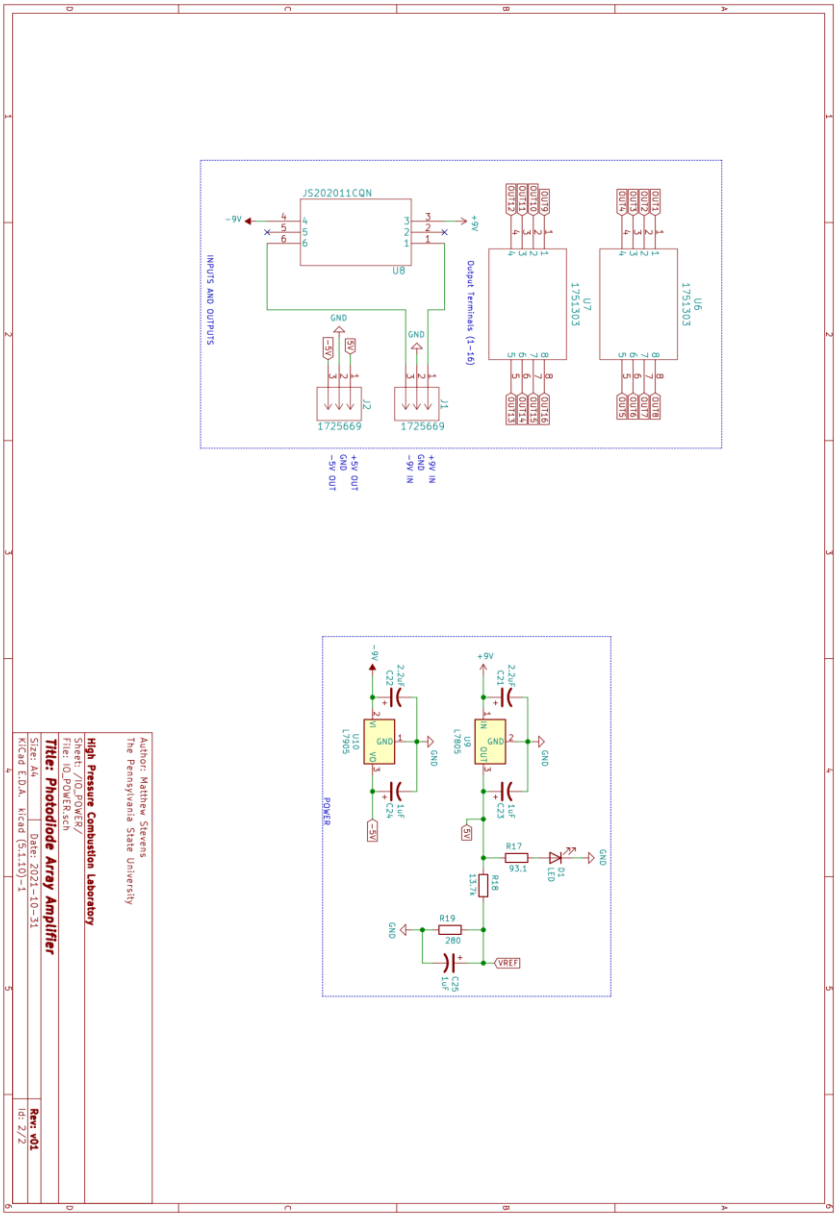

Figure 33. Amplification PCB Schematic Pg.2

Appendix B MATLAB Post Processing Code

```
% Photodiode Array Post-Processing Program
% Matthew Stevens
% 3/23/2022
%
% This program calculates the burning rate of solid propellants using voltage-time data from a
photodiode array.
% Strand burner uses InstruNet i100, and stock software for data aquisition. Time column in sec.
clear, clc;
close all force;     %Force closes all plots

%%adding libraries to path
addpath('\\udrive.ad.psu.edu\Users\m\j\mjs7660\Desktop\HPCL\v1.6 Photodiode Data
Recording\PlotPubLibraryFiles');

%% Constants
global numDiodes diodeSpacing timeVector;  %%defining some vars global so can be used in
function
numDiodes = 11;            %number diode channels in data file
diodeSpacing = 0.0625;      %in. distance between centers of each diode on the array
sampleTime = 1000;          %hz Only needed for LabView program. Not need for strand burner
DAQ setup
%value_threshold = 0.15;       %%%%%V. Value when threshold will be marked. Used for
threshold-based rate calc
velLimit = 10000;             %in/2. Max value of velocity allowable. All greater values will be not
included in rate calcs.
span = 50;                %Number of points used in the moving average

%Time Trim Constants
cushionBack = 2.0;            %num sec before start of burn and after end of burn to plot
cushionFront = 3.2;
threshold_trim = 0.15; %volage to start and end time trim at

% Flags to turn on/off functions
timeTrimFlag = 0;  %0 for no trim. 1 for trim. To trim time around burn to focus on area of
intrest. Use time trim constants above.
curveFitTrailFlag = 0;

%Polynomial Fit Constants
threshold = 0.15; %value below which bounds of polynomial time axis are set by.
polyOrder = 2;   %Order of polynomial fit

%% Importing Labview Data File
```

```
disp('Choose data file (Save .lvm as a .txt file first, and delete rows up until data starts. (Ensure file is in the same directory!, Check Sample Time!):')
filename = uigetfile('*.txt','Select a file');
disp(filename); %Displaying the file name selected
dataMatrix = importdata(filename);
timeVector = dataMatrix(:,1); %Converting Time Column to s
dataMatrix(:,1) = []; %Deleting Time column from dataMatrix       old
%dataMatrix(:,2:numDiodes+1);

%dataMatrix(:,1) = [];  %%%%%%%%%%deleting data from first diode TEMPPORARY for test 5

%timeVector = timeVector/1000;   only use for data from SCB-68 DAQ
%% Trimming Data to Only Region of Interest for plotting
if (timeTrimFlag==1)

   [~,indexFirst]=min(dataMatrix(:,round((numDiodes/2),0)));   %looking at central diode. Finding minimum. Adding cushion to either side

   %indexFirst = find(dataMatrix(:,2)<threshold_trim,1,'first');  %finding first index where voltage output is less than threshold
   %indexLast = find(dataMatrix(:,2)<threshold_trim,1,'last');  %finding last index where voltage output is less than threshold

   cushionIndex_start = find(timeVector>timeVector(indexFirst)-cushionBack,1,'first'); %finding first time index greater than Time(indexFirst)-cushion. Will be equal to first point of action minus the cushion time
   cushionIndex_end = find(timeVector>timeVector(indexFirst)+cushionFront,1,'first'); %finding first time index greater than Time(indexLast)+cushion. Will be equal to last point of action plus the cushion time

   timeOffset = timeVector(cushionIndex_start);            %value to offset time data by

   timeVector = timeVector(cushionIndex_start:cushionIndex_end); %Trimming time vector to just space within indices
   dataMatrix = dataMatrix(cushionIndex_start:cushionIndex_end,:);

   timeVector(:) = timeVector(:)-timeOffset;      %offsetting timevector by first index time value. Resets to zero time.
end

%% Plotting Raw Voltage Outputs
Figure(1)
pointSpacing = 20;
```

```
for i=1:1:numDiodes
   plot(timeVector(1:pointSpacing:end),dataMatrix(1:pointSpacing:end,i))
   hold on
end
grid on;

xlabel('Time (s)');
ylabel('Voltage (V)');
legend("Diode 1","Diode 2","Diode 3","Diode 4","Diode 5","Diode 6","Diode 7","Diode
8","Diode 9","Diode 10","Diode 11",'Location','southeast','NumColumns',1)
hold off;

%Parameters for modifying the current Figure
opt = [];
opt.BoxDim = [6,6];
opt.LegendBox = 'off';
opt.Resolution = '600';
% update the current plot
setPlotProp(opt); %modifies the existing plot

%% Smoothing Data With Moving Average. Derivative Calc
for i=1:1:numDiodes %stepping through each diode in Matrix. Column=i
   %smoothing Data
   dataMatrix_Smooth(:,i) = smooth(dataMatrix(:,i),span); %smoothing raw voltage-time data.
MATLAB function.
end

%% Threshold Rate Calc (Looking at when each diode crosses a certain threshold voltage value)
% First determine range of threshold value to try:
for i=1:1:numDiodes
   minVector(i) = min(dataMatrix_Smooth(:,i));  %finding minimums of each channel
   maxVector(i) = max(dataMatrix_Smooth(:,i));  %finding max of each channel
end
thresholdLowerBound = max(minVector);  %ensuring that lowest val taken for threshold is
something attainable by all channels...
thresholdUpperBound = min(maxVector);  %ensuring that upper val taken for threshold is
something attainable by all channels...

thresIncrement = 0.001;%increment to go by on each threshold
j=0;
for currentThres=thresholdLowerBound:thresIncrement:thresholdUpperBound
   j=j+1;
   [R_Sq(j),leastsquares_avgRate(j)] = thresholdRateFunct(currentThres,dataMatrix_Smooth);
%returns R_Sq value and rate for each threshold
```

```
   thresholds(j) = currentThres;
end

[maxR_sq,maxR_SqIndex] = max(R_Sq);
finalThreshold = thresholds(maxR_SqIndex);                    %returning threshold value
cooresponding to greatest R^2 value
leastsquares_avgRate_final = leastsquares_avgRate(maxR_SqIndex);  %returnig rate value
cooresponding to greatest R^2 value
fprintf("\nThreshold, Least-Squares = \n     %.3f in/s \n     %.3f cm/s
\n",leastsquares_avgRate_final,leastsquares_avgRate_final*2.54)
fprintf("     R^2 = %.3f\n",maxR_sq);
fprintf("     Threshold = %.3f V\n",finalThreshold);

%% Plotting Smoothed Data, including markers of optimal thresholdd
% first get markers for where thresholds are crossed on each plot
for i=1:1:numDiodes %stepping through each diode in Matrix. Column=i
   value_threshold_markers(i) = find(dataMatrix_Smooth(:,i)<=finalThreshold,1); %finding first
value under value theshold.
end
Figure(2)
grid off;
hold on;
%title('Photodiode Array Outputs');
xlabel('Time (s)');
ylabel('Voltage (V)');
for i=1:1:numDiodes
   plot(timeVector,dataMatrix_Smooth(:,i));
end

%Getting colors
% Create 10 data series
XY = rand(11);
% Build colormap and shuffle
cmap = colormap(turbo(size(XY,2)));
colororder(cmap);

%plotting points on plot where thresholds were first crossed
for i=1:1:numDiodes

plot(timeVector(value_threshold_markers(i)),dataMatrix_Smooth(value_threshold_markers(i),i),
'k.','MarkerSize',30);
end
```

```
legend("Diode 1","Diode 2","Diode 3","Diode 4","Diode 5","Diode 6","Diode 7","Diode
8","Diode 9","Diode 10","Diode 11","Threshold",'Location','southeast','NumColumns',1)
%,"Diode 10"
hold off;

%%%%%%%%%%%%%%%%%%%%%%%%%%%%%%%%%%%%%%%%%%%%%
%%%%
%Parameters for modifying the current Figure
opt = [];
opt.BoxDim = [6,6];
opt.LegendBox = 'off';
opt.Resolution = '600';
setPlotProp(opt); %modifies the existing plot
%%%%%%%%%%%%%%%%%%%%%%%%%%%%%%%%%%%%%%%%%%%%%
%%%%

%% Plotting Position-Time. First diode is origin (x=0)
x = 0:diodeSpacing:diodeSpacing*(numDiodes-1); %in. Position of light source when minimum
is reached on each channel.
%Position-time for threshold rate
minTimes = timeVector(value_threshold_markers(:));   %returns time of eacch minimum from
threshhold
p = polyfit(minTimes,x',1); %returns coefficient of first order polyninomial fit (linear
regression). p(1) is slope. p(2) is y-intercept
f = polyval(p,minTimes);    %evaluating p polynomial at each point in minTimes
Figure(3)
plot(minTimes,x,'ko',minTimes,f,'k-')
grid off;
%title('Burning Surface Position');
xlabel('Time (s)');
ylabel('Position (in)');
legend("Burning Surface Position","Linear Fit",'Location','southeast')

%%%%%%%%%%%%%%%%%%%%%%%%%%%%%%%%%%%%%%%%%%%%%
%%%%
%Parameters for modifying the current Figure
opt = [];
opt.BoxDim = [6,6];
opt.LegendBox = 'off';
opt.Resolution = '600';
%opt.Markers = {'o', '', 's'};
%opt.MarkerSpacing = [50, 50, 50];
% update the current plot
setPlotProp(opt); %modifies the existing plot
```

```
%%%%%%%%%%%%%%%%%%%%%%%%%%%%%%%%%%%%%%%%%%%%%
%%%%

%% Old rate calc methods
for i=2:1:numDiodes
   v_threshold(i)= diodeSpacing / (timeVector(value_threshold_markers(i))-
timeVector(value_threshold_markers(i-1)) ); %in/s
end

%threshold average rate
v_threshold(:,1) = []; %deleting first column, which is zero
v_avg__threshold = mean(v_threshold);
fprintf("\nThreshold-Based Rate, average = \n     %.3f in/s \n     %.3f cm/s
\n",v_avg__threshold,v_avg__threshold*2.54)

% Determining rate based on the entire array length...
v_threshold_totalLength = (numDiodes*diodeSpacing) /
(timeVector(value_threshold_markers(numDiodes))-timeVector(value_threshold_markers(1)) );
fprintf("\nThreshold-Based Rate, entire array = \n     %.3f in/s \n     %.3f cm/s
\n",v_threshold_totalLength,v_threshold_totalLength*2.54)

%% Plotting R^2 vs threshold values
Figure(4)
grid off;

yyaxis left
plot(thresholds,R_Sq,'k-','LineWidth',3); % plotting R^2 on left axis
ylabel('R^2','Color','k');
ax = gca;
% This sets background color to black
ax.Color = 'k';
ax.YColor = 'k';

yyaxis right
plot(thresholds,leastsquares_avgRate,'k--','LineWidth',3);
ylabel('Calculated Rate (in/s)');

%title('Change in Regression fit with Threshold Values');
xlabel('Threshold (V)');
legend("R^2 Value","Burning Rate",'Location','southwest');

%%%%%%%%%%%%%%%%%%%%%%%%%%%%%%%%%%%%%%%%%%%%%
%%%%
%Parameters for modifying the current Figure
```

```
opt = [];
opt.BoxDim = [6,6];
opt.LegendBox = 'off';
opt.Resolution = '600';
opt.HoldLines = 'True';
opt.AxisColor = 'black';
%opt.LineWidth = [5,5];
% update the current plot
setPlotProp(opt); %modifies the existing plot
%%%%%%%%%%%%%%%%%%%%%%%%%%%%%%%%%%%%%%%%%%%%
%%%%

%% Data Output as CSV
fprintf("\n%.3f,%.3f,%.3f,%.3f,%.3f
\n",leastsquares_avgRate_final,v_avg__threshold,v_threshold_totalLength,finalThreshold,maxR
_sq);

%% Curve Fitting to Trailing edges of Burn
if (curveFitTrailFlag == 1)
   polyOrder = 1;
   initialTime = 2.6*1000; % for poly fit
   endTime = 4.3*1000;  % fot poly fit
   k = 9;    %diode to fit against
   realDataOffset = 0.5*1000;   %to plot a little more for visibility

   trimTimeVect = timeVector(initialTime:endTime);
   trimDiodeVect = dataMatrix_Smooth(initialTime:endTime,k);

   p = polyfit(trimTimeVect,trimDiodeVect,polyOrder);
   f = polyval(p,trimTimeVect);    %evaluating p polynomial at each point in timevector

   Figure(5)
   plot(timeVector(initialTime-
realDataOffset:(endTime+realDataOffset)),dataMatrix_Smooth(initialTime-
realDataOffset:endTime+realDataOffset,k),'k:',trimTimeVect,f,'k-');
   grid off;
   %title('Burning Surface Position');
   xlabel('Time (s)');
   ylabel('Voltage (V)');
   legend("Diode 9",['V = ',num2str(round(p(1),4)),'t + ',num2str(round(p(2),4))]); %,'t +
',num2str(round(p(3),4))],'Location','southeast');
   %annotation('textbox',[0.6 0.3 .2 .2],'String',['V = ',num2str(round(p(1),4)),'t^2 +
',num2str(round(p(2),4)),'t + ',num2str(round(p(3),4))],'FitBoxToText','on');
```

```
    %yfit = p(1)*x + p(2); %position value at each minTime for the regression curve


%%%%%%%%%%%%%%%%%%%%%%%%%%%%%%%%%%%%%%%%%%%
%%%%
    %Parameters for modifying the current Figure
    opt = [];
    opt.BoxDim = [6,6];
    opt.LegendBox = 'off';
    opt.Resolution = '600';
    % update the current plot
    setPlotProp(opt); %modifies the existing plot

%%%%%%%%%%%%%%%%%%%%%%%%%%%%%%%%%%%%%%%%%%%
%%%%
end



%% Function for computing R^2 value at a threshold.
% Inputs:
%   threshold value - value where photodiode outputs will be marked for calculating rate
%   dataMatrix_Smooth - matrix of photodiode outputs after being smoothed (calculated
previously)
% Outputs:
%   R_sq - R^2 value relating to how well data fits to line. This value is minimized by choosing
best threshold
%   leastsquares_avgRate - the rate determined from best fit line
function [R_Sq,leastsquares_avgRate] = thresholdRateFunct(threshold,dataMatrix_Smooth)
    global numDiodes diodeSpacing timeVector;
    for i=1:1:numDiodes %stepping through each diode in Matrix. Column=i
        value_threshold_markers(i) = find(dataMatrix_Smooth(:,i)<=threshold,1); %finding first
value under value theshold for each channel
    end
    %Linear regression based on x-t
    positions = 0:diodeSpacing:diodeSpacing*(numDiodes-1); %in. Position of light source when
minimum is reached on each channel.
    minTimes = timeVector(value_threshold_markers(:));   %returns time of each minimum from
threshhold
    p = polyfit(minTimes,positions',1); %first order polyninomial fit (linear regression)

    leastsquares_avgRate = p(1);  %slope equal to first term in polynomial fit coefficients

    %computing R^2 value
```

```
    x = minTimes;  %redefining for readability
    y = positions';
    yfit = p(1)*x + p(2); %position value at each minTime for the regression curve
    RSS = sum((y-yfit).^2);  %residual sum of squares. Squaring difference between fit curve and
actual data at each x. Then summing
    TSS = (length(y)-1)*var(y); %Total sum of squares. involves variance of y
    R_Sq = 1-RSS/TSS;
end
```

Appendix C A2V-16 Photodiode Array Datasheet

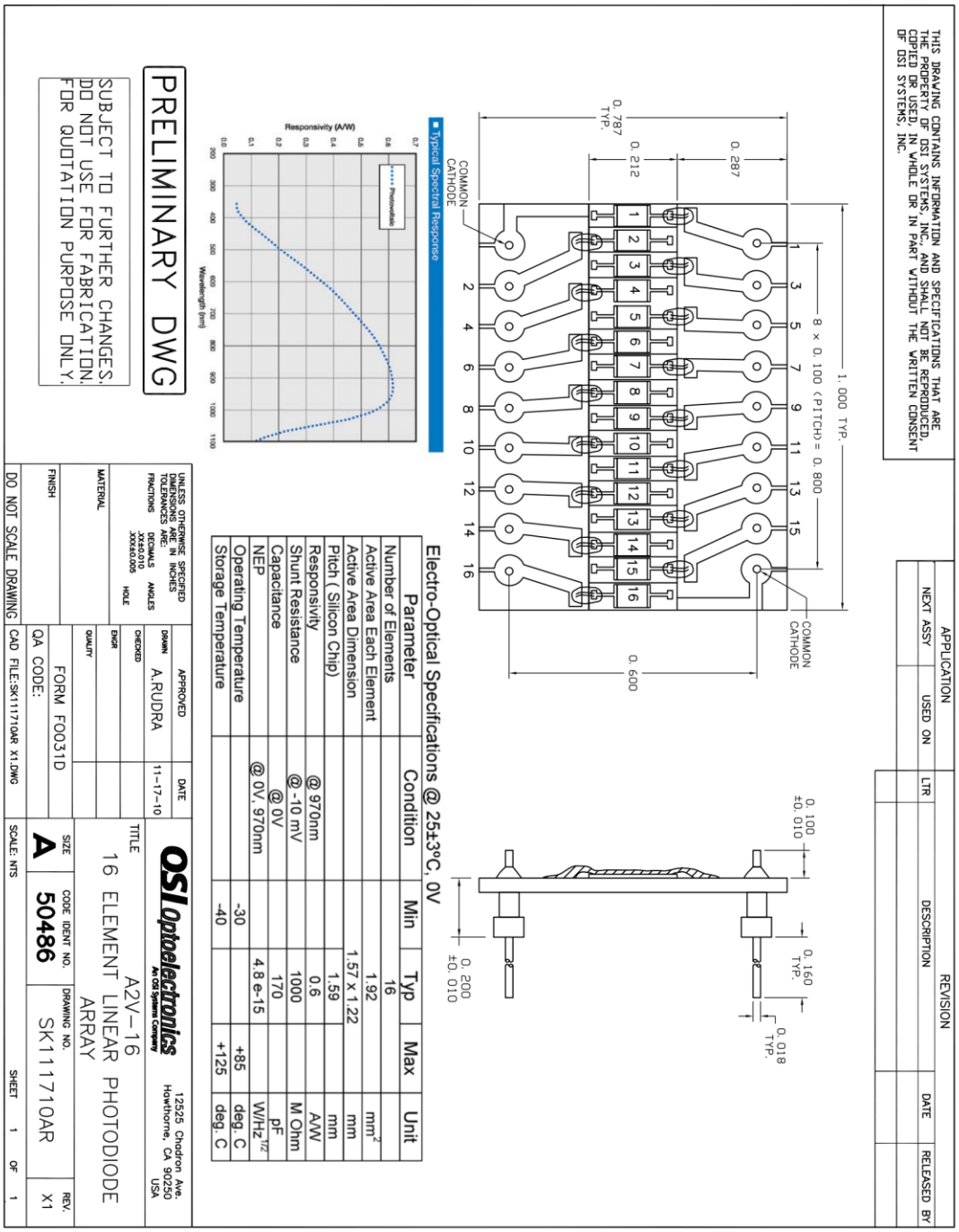

Figure 34. A2V-16 Photodiode Array data sheet

Appendix D Linear Actuator Test Data

Table 2. Linear Actuator Test Results

Actuator Speed (in/s)	Calculated Speed from Photodiodes (in/s)	Difference (in/s)	% Difference
1.21	1.027	0.183	16.36%
0.91	0.757	0.153	18.36%
0.73	0.615	0.115	17.10%
0.61	0.514	0.096	17.08%

The linear actuator-calculated speed differed fairly significantly form the rate determined by the photodiode array. This is likely due to lag in the movement of the linear actuator from when the Arduino Microcontroller gave the command to move. The actuator did provide positional feedback, so it was assumed that when the Arduino stopped commanding the servo to move it immediately stopped moving. This rough assumption, coupled with startup and stop transients of the actuator movement likely led to the larger differences inTable6. Additionally, the differences seem to increase with increasing speeds, which is expected, as the actuator will take longer to speed up, hence reducing its actual overall speed.

Although the actuator speed was not precisely known, it still served to validate the photodiode circuitry and post processing code in a desk-top environment before moving on to strand burner tests.

Appendix E Tests to Determine Amplifier Gain

The first 4 strand burner tests were used to determine the appropriate gain value for the transimpedance amplifiers. A gain that was too high would saturate the +/-5V input on the data acquisition system while too low of a gain would not produce a readable voltage level. Radiance data on the ASRM propellant was not readily available, so an experimental approach was used for determining the correct gain value.

A gain of -11V/mA, corresponding to an 11k ohm resistor, was initially used and tested with the ASRM propellant at 100psi. This gain was initially used with linear actuator and LED to validate the system, and was expected to be too high for the ASRM propellant but would serve as an upper limit. Figure 35 shows the voltage outputs of the photodiodes at this gain.

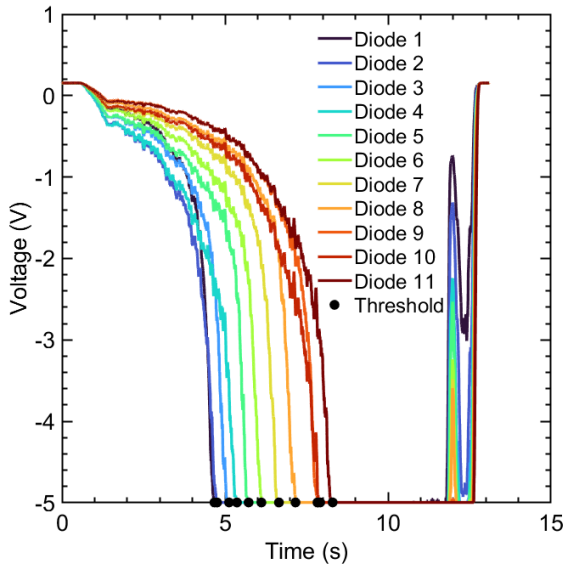

Figure 35. ASRM propellant burn at 100psi with -11 V/mA gain.

Around the 1 second mark the voltage outputs already begin to respond to the initialization of the propellant burning, before the burning surface has passed. By the 5 second mark, the first couple diodes have saturated the voltage input of the InstruNet Data Acquisition

system, indicating that the gains are too high. Although much of the signal was lost due to being out of the input range of the data acquisition module, a reasonable burning rate 0f 0.155 in/s was still determined, agreeing closely with the camera-measured rate.

A final gain value of -0.1V/mA, corresponding to a 100ohm feedback resistance, was determined to work well for the ASRM propellant. Figure 36 shows the output curve from the photodiodes for a 100 psi burn at this gain level.

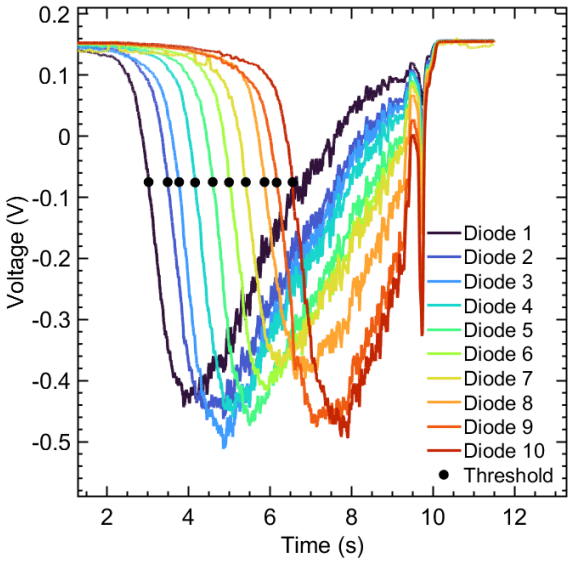

Figure 36. ASRM propellant burn at 100psi with -0.1 V/mA gain

Although the voltage outputs do not fill the entire +/-5V input range of the data acquisition module, the resolution was still acceptable for determining burning rates.

References

[1] Thynell, S. T., Huang, I. T., Kuo, C. S., Hsieh, W. H., Kuo, K. K. "Approach to Measurements of Flame Spreading over Solid Propellants." *Journal of Propulsion and Power*, vol. 8, no. 4, 1992, pp. 914–917.

[2] Fry, R. S., DeLuca, L., Frederick, R., Gadiot, G., Strecker, R., Besser, H-L., Whitehouse, A. Traineau, J-C., Ribereau, D., Reynaud, J-P. "Evaluation of Methods for Solid Propellant Burning Rate Measurement." 2002.

[3] Kuo, K. "Transient Burning Characteristics of JA2 Propellant Using Experimentally Determined Zel'dovich Map (Invited)." 39th AIAA/ASME/SAE/ASEE Joint Propulsion Conference and Exhibit, 2003.

[4] G. Sutton, Rocket Propulsion Elements, 6th ed., New York, NY: John Wiley and Sons, Inc., 1992.

[5] Landers, L., Booth, D. W., Stanley, C. B., Ricks, D. W. "ASRM Propellant and Igniter Propellant Development and Process Scale-Up." 29th Joint Propulsion Conference and Exhibit, 1993.

[6] Q. Niu, Z. He, S. Dong, IR radiation characteristics of rocket exhaust plumes under varying motor operating conditions, *Chinese J. Aeronaut*. 30 (2017) 1101–1114.

[7] Min Taek Kim, Soonho Song, Yoo Jin Yim, Myung Wook Jang, Gookhyun Baek. "Comparative Study on Infrared Irradiance Emitted from Standard and Real Rocket Motor Plumes." *Propellants, Explosives, Pyrotechnics*, vol. 40, no. 5, 2015, pp. 779–785.

[8] Fry, Ronald S. "Solid Propellant Subscale Burning Rate Test Techniques and Hardware for U.S. and Selected NATO Facilities." 2001.

[9] Gupta, Garima, Jawale, Lalita, Bhattacharya, Bikash. "Various Methods for the Determination of the Burning Rates of Solid Propellants - An Overview." *Central European Journal of Energetic Materials*, 2015, pp. 593–620.

[10] Osborn, J. R., Murphy, J. M., Kershner, S. D. "Photographic Measurement of Burning Rates in Solid Propellant Rocket Motors." *Review of Scientific Instruments*, vol. 34, no. 3, 1963, pp. 305–306.

[11] Sippel, Travis R. "Characterization of Nanoscale Aluminum and Ice Solid Propellants." Purdue University [Masters Dissertation], 2009.

[12] Caldwell, John. "Transimpedance Amplifiers: What Op Amp Bandwidth Do I Need?" *Precision Hub - Archives - TI E2E Support Forums*,

https://e2e.ti.com/blogs_/archives/b/precisionhub/posts/part-iii-what-op-amp-bandwidth-do-i-need-transimpedance-amplifiers, May 7, 2014.

[13] “Online Circuit Simulator & Schematic Editor.” CircuitLab, https://www.circuitlab.com/. Accessed 1 Apr. 2022.

[14] Cohen, Dan. “Solid Propellant Regression Measurements Using Imbedded Chemical Tracers AND Design of Test Program and Facilities for Investigation of the Erosive Burning and Flame Spreading Characteristics of the Solid Propellant Used in Advanced Solid Rocket Motors (ASRM).” The Pennsylvania State University [Masters Dissertation], 1994.

[15] “High Pressure Combustion Lab.” *PSU HPCL*, http://www.hpcl.psu.edu/. Accessed 1 Apr. 2022.

Academic Vita

MATTHEW J. STEVENS

mjs7660@psu.edu | MatthewJamesStevens.com

EDUCATION

Schreyer Honors College | **The Pennsylvania State University** *Expected: May 2022*

B.S. Aerospace Engineering

ENGINEERING EXPERIENCE

SpaceX – Starship Engineering Intern *Brownsville, TX | May-August 2021*

- Designed and manufactured a torque frame install tool for the flap primary structures on the Starship Orbital launch vehicle (S21 onward)
- Designed back purge boxes with vacuum suction to prevent oxidation of 304L welds on Starship. Rolled out 4 units for use on the factory floor of the nosecone production line
- Ran weld test matrices to determine the strength knockdown of oxidized welds at cryogenic temperatures, and the required argon backpurge levels to prevent sugaring of 304L welds

Penn State, High Pressure Combustion Lab – Research *State College, PA | May 2021 - Present*

- Conducting honors thesis work to design a photodiode array system to measure burning rates of solid rocket propellant
- Designing a photodiode array system, making custom circuitry to amplify diode outputs, writing code to calculate burning rate from changes in diode output currents

PSU SEDS Liquid Rocket Team – Project Manager *State College, PA | January 2019-Present*

- Leading 30-member team to design and test an 800lbf bi-propellant rocket engine and test stand
- Completed hand calculations and FEA on engine components, created programs to predict rocket trajectory with drag, determined required engine thrust levels and propellant mass, designed engine and nozzle using isentropic flow equations and NASA's CEA program
- Lead meetings and help team members learn about rocket engine and test stand design

SpaceX – Starlink Intern *Hawthorne, CA | May-August 2020*

- Created the installation process and tooling for the radome on the first public beta Starlink user terminals. Improved throughput yield multiple percentage points to above 98%
- Implemented light curtain safety closeouts for a 24m span of curing presses
- Designed an elevator and indexer for Starlink user terminal pallets on the factory assembly line

Skillman Rocketry Company – Founder (skillmanrocketry.com) *May 2019 – August 2021*

- Formed a research and development company selling test equipment for solid rocket motors

- Designed a thrust stand and data acquisition electronics to collect high sample rate pressure and thrust data from mid to high power motors. Brought products to market
- Designed and tested a solid rocket motor for 30 test fires with a 124s I_{sp}, 390N max thrust, and 750psi max pressure
- Created MATLAB and Python programs to generate predicted thrust and pressure curves, designed nozzle, analyzed motor design, and evaluate thermal and structural constraints

SES Satellites – Payload Engineering Intern *Princeton, NJ | May-August 2019*

- Wrote Python code to process data from the AMC-15/AMC-16 satellites and display which downlink and receiver are currently paired using a GUI
- Automated the creation of telemetry display pages with an intuitive website using HTML, CSS, and JavaScript to save hours of time required to manually update pages

SKILLS

Programming: MATLAB, C++, Python, HTML/CSS/JavaScript, Arduino, NASA CEA

Technical: Siemens NX, SOLIDWORKS, ANSYS, NASA CEA, Fusion 360, EAGLE, KiCad, circuitry, pneumatics

AWARDS

NASA PSGC Undergraduate Scholarship May 2021

Admission to the Schreyer Honors College for Aerospace Engineering June 2019

The Rawson Group Scholarship for Aerospace Engineering June 2018